Synthesis of Multi-constraint Adaptive Antenna Array Employing Harmony Search and Differential Evolution Techniques

Dondapati Suneel Varma

Department of Electrical Engineering
National Institute of Technology,Rourkela
Rourkela-769008, Odisha, INDIA
May 2013

Synthesis of Multi-constraint Adaptive Antenna Array Employing Harmony Search and Differential Evolution Techniques

A thesis submitted in partial fulfillment of the
requirements for the degree of

Master of Technology

in

Electronics Systems and Communication

by

Dondapati Suneel Varma
(Roll-211EE1098)

Under the Guidance of

Prof.K. R. Subhashini

Department of Electrical Engineering
National Institute of Technology,Rourkela
Rourkela-769008, Odisha, INDIA
2011-2013

Department of Electrical Engineering

National Institute of Technology, Rourkela

CERTIFICATE

This is to certify that the thesis entitled ***"Synthesis of Multi-constraint Adaptive Antenna Array Employing Harmony Search and Differential Evolution Techniques"*** *by* ***Mr. DONDAPATI SUNEEL VARMA****, submitted to the National Institute of Technology, Rourkela (Deemed University) for the award of Master of Technology in Electrical Engineering, is a record of bonafide research work carried out by him in the Department of Electrical Engineering , under my supervision. I believe that this thesis fulfills part of the requirements for the award of degree of Master of Technology. The results embodied in the thesis have not been submitted for the award of any other degree elsewhere.*

Place:Rourkela

Date:

Prof.K. R. Subhashini

To My Loving PARENTS and Inspiring GUIDE

Acknowledgements

First and foremost, I am truly and heartyfully indebted to my supervisors Professor K. R. SUBHASHINI for their inspiration, excellent guidance and unwavering confidence through my study, without which this thesis would not be in its present form. I also thank them for their gracious encouragement throughout the work. I express my gratitude to the faculties, Professors D. PATRA, S. DAS, P. K. SAHOO, K. R. SUBHASHINI for their advise and care during internal evaluation. I am also very much obliged to Prof. A.K.Panda Head of the Department of Electrical Engineering, NIT Rourkela for providing all the possible facilities towards this work. Thanks also to other faculty members in the department. I would like to thank A TOSHIBA PRAVEEN KUMAR, for support and suggestions towards the work and a great company during problem solving situations. I would like to thank ARAVIND PUTTUPU and OBULESU DANDU , NIT Rourkela, for their enjoyable and helpful company I had with. I would like to thank AYAN KANTI SANTRA who helped me to know about the software Latex. Last but not least my wholehearted gratitude to my parents, KIRAN KUMAR and RATNA JYOTSNA, for their encouragement and support.

DONDAPATI SUNEEL VARMA

Rourkela, MAY 2013

Contents

Abstract

Smart Antenna systems have recently received increasing interest as the demand for better quality and new value added services on the existing wireless communication systems. There is a great increase in demand on mobile wireless operators to provide voice and high-speed data services and to support more users per base station in order to reduce overall network costs and make the services affordable to subscribers. Smart antenna technology offers a significantly improved solution to reduce interference levels and improve the system capacity. These system of antennas include different geometry and adaptive techniques to enhance the received signal with a fixed DOA by suppressing the interferences. Although enormous study has been done on smart antennas special emphasis and development has not been provided to the antenna array structure and adaptive methods. In this work a scheme attempt is made to use a met-heuristic musical inspired Harmony Search (HS) algorithm and Differential Evolution technique to formulate the adaptive equations and to detect the Angle of arrival and angle of interference with multiple users. Comparative analysis of the two techniques is performed.

List of Figures

List of Tables

List of Abbreviations

Abbreviation	Description
AF	Array Factor
DEA	Differential Evolution Algorithm
HS	Harmony Search
DOA	Direction Of Arrival
AOA	Angle Of Arrival
AOI	Angle Of Interference
IHS	Improved Harmony Search
HMS	Harmony Memory Size
HMCR	Harmony Memory Considering Rate
PAR	Pitch Adjusting Rate
FCM	Fuzzy C-Mean

Chapter 1

INTRODUCTION

1.1 Introduction

Over the last few years demand for service provision via the wireless communication bearer has risen beyond all expectations. If the extra ordinary fact that worldwide some half a billion subscribers to mobile networks are predicted by the year 2000 is put in the context of third generation system requirement, then the most demanding technological challenge emerges, there is a need to increase the spectrum efficiency of wireless networks[1]. While great effort in current generation wireless communication system has been directed toward the development of modulation, coding and protocol, antenna-related technology and terminology has received significantly less attention till now. To achieve the ambitious requirements introduced for future wireless systems new intelligent or self-configured and highly efficient systems will most certainly be required. In the pursuit of schemes that will solve these problems, recently attention has turned to spatial filtering methods using advanced antenna techniques, adaptive or smart antennas using different adaptive array structures [2][3]. Spatial dimension can be exploited as a hybrid multiple-access technique complementing TDMA, FDMA and CDMA. Possibly the most challenging problem related to smart antennas is their practical implementation. Full exploitation of all the operational benefits would mean increased complexity for the system and hence would require

a fully integrated approach in an intelligent system. RF and DSP have to evolve furthermore before this can be achieved in a cost effective manner.

1.2 Literature review

For improving the capacity of the base station in wireless communication we need a antenna system which focus the radiated electro magnetic energy for improving the gain pattern[4]. One of the antenna model which suits above situation is Smart antenna. A smart antenna is a phased or adaptive array that adjusts to the environment. That means, for the adaptive array, the beam pattern changes as the desired user and the interference moves, and for the phased array, the beam is steered or different beams are selected as the desired user moves. Main beam steering is not the only core technology of smart antenna but it can effectively reduce the multi-path interference and minimize the multi-path effect[5]. Different geometries of the adaptive antenna or smart antenna array are mentioned by El Zooghby, Ahmed in [3]. In an array the analysis is done by considering the first element as the phase reference element[6]. The objective function for the smart antenna synthesis is formed by Zaharis, Zaharias D and Skeberis, Christos and Xenos, Thomas D [7].

Many approaches have been proposed to make the adaptive beam former. For the typical array imperfection,i.e., DOA estimation, many solutions have been proposed, such as convex quadratic constraints, Bayesian approach and uncertainty set based method. All these methods belong to a class of popular robust beam forming methods, the diagonal loading method. However, the selection of the optimal diagonal loading level is still not clear in practice[8]. For that reason evolutionary algorithms have been applied to the adaptive beam forming problem which are inspired by the natural evolution of species. When implementing the EAs, user not only need to determine the appropriate encoding schemes and evolutionary operators, but also need to choose the

suitable parameter settings to ensure the success of the algorithm, which may lead to demanding computational costs due to the time-consuming trial-and-error parameter and operator tuning process[9]. More recently, differential evolution method is simple and powerful optimization technique[10]. A differential evolution algorithm is an evolutionary computation method that was originally introduced by Storn and Price in 1995[11][12][13]. Furthermore, they 29 developed DEA to be a reliable and versatile function optimizer that is also readily applicable to a wide range of optimization problems. The effectiveness of conventional DE in solving a numerical optimization problem depends on the selected mutation and crossover strategies and their associated parameter values[14].

One of the recently developed evolutionary algorithm conceptualized using the process of getting a perfect state of harmony by the musicians. Geem developed a new harmony search (HS) meta-heuristic algorithm that inspired from the musicians in 2001[15]. The harmony in music is analogous to the optimization solution vector, and the musicians improvisations are analogous to local and global search schemes in optimization techniques. The HS algorithm does not require initial values for the decision variables[16]. The HS algorithm has a novel stochastic derivative (for discrete variable) based on musicians experience, rather than gradient (for continuous variable) in differential calculus[17]. In optimization each decision variable initially chooses any value within the possible range, together making one solution vector. If all the values of decision variables make a good solution, that experience is stored in each variables memory, and the possibility of making a good solution is also increased next time. When a musician improvises one pitch, he (or she) has to follow some rules[18]. In HS tuning of controlling parameters are very important to obtain the optimal solution[19]. For the tuning of parameter some modifications has been proposed. In 2007 a modification is occurred in HS[19] after that global best HS was proposed[20]. In the modification the modification is done in the creation of new harmony. Lucas M.

Pavelski extended the use of HS to the multi-objectives[21].

1.3 Objectives

The objective of the thesis is to design the smart antenna array by employing Differential Evolution (DE) and Harmony Search (HS) which are in the class of evolutionary techniques. Smart antennas are the antenna systems which can steer the main beam towards the desired direction called direction of arrival (DOA) and minimizing the intensity level at the interference angles. Now the objective is viewed as two main constraints steering the main beam and other for minimizing the intensity at the interference level. The cost/objective function is formulated as an optimization task, in that care of the angle of arrival (AOA) θ_0 and other for angle of interference (AOI) $\theta_n(n = 1, ...N)$. The objective function is designed to have the weighted summation of different constraints in the presence of additive zero-mean Gaussian noise with variance σ^2_{noise} given by.[7]

$$\overline{w} = [w_1\ w_2\ w_3\ .\ .\ w_M]^T$$

$$\overline{A} = [\overline{a}_1\ \overline{a}_2\ \overline{a}_3\ .\ .\ .\overline{a}_N]$$

$$\overline{a}_n = [1 \exp^{j\frac{2\pi}{\lambda}q\sin\theta_n}\ .\ .\ \exp^{j(M-1)\frac{2\pi}{\lambda}q\sin\theta_n}]$$

In the above equations $\overline{w}$ indicates number of users, $\overline{A}$ represents an array which is dependent on the number of interference angles and $\overline{a}_n$ indicates the array factor.

$$F_1 = \frac{\overline{w}^H\overline{A}\overline{A}^H\overline{w}}{\overline{w}^H\overline{a_0}\overline{a_0}^H\overline{w}}$$

$$F_2 = \frac{\sigma^2_{noise}\overline{w}^H\overline{w}}{\overline{w}^H\overline{a_0}\overline{a_0}^H\overline{w}}$$

Where F_1 is partial objective for steering the main beam towards the DOA and F_2 is sub function is to minimize the intensity level at the interference angle. Summation of both objective function will takes care of the chosen

objectives

$$F = F_1 + F_2$$

1.4 Thesis Organization

The thesis is organized as follows.

- In chapter 2, Smart antenna and different geometries i.e. linear and circular geometries are discussed. Along with that the objective function formulation is also described.
- Chapter 3 gives the overview of the evolutionary algorithms for adaptation proposed algorithms and modifications.
- In Chapter 4, concludes the thesis. Extension of the present work and future scope for further work are also discussed there.

Chapter 2

SMART ANTENNA SYSTEM

2.1 SMART ANTENNA

An antenna can be described as a structure made of material bodies that can be composed of either conducting or dielectric materials or a combination of both. The structure should be matched to the source of the electromagnetic energy so that it can radiate or receive the electromagnetic fields in an efficient manner[4]. One of the recent antenna which gained popularity is the Smart antenna. In reality, antenna systems are smart not the antenna. Generally collocated with a base station, a smart antenna system combines to form an antenna array with a digital signal-processing capability to transmit and receive in an adaptive and spatially sensitive manner. This type of system can automatically change the direction of its radiation patterns in response to its signal environment. This can improve the performance characteristics (such as capacity) of a wireless system.

A smart antenna is a phased or adaptive array that adjusts to the environment. That means, for the adaptive array, the beam pattern changes as the desired user and the interference position varies, and for the phased array, the beam is steered or different beams are selected depending on the position of the user. A smart antenna system combines multiple antenna elements with a signal processing capability to optimize its radiation and/or reception pattern in response to the signal environment automatically. Smart antenna

systems are customarily categorized as either switched beam or adaptive array systems.

There are mainly two categories in smart antenna system they are SWITCHED BEAM ANTENNAS and ADAPTIVE BEAM ANTENNAS.

Switched beam antenna system form multiple fixed beams with amplified/magnified sensitivity in particular directions. These antenna systems detect signal strength, choose from one of several predetermined, fixed beams, and switch from one beam to another as demand changes throughout the sector. Instead of shaping the directional antenna pattern with the metallic properties and physical design of a single element (like a sectionized antenna), switched beam systems combine the outputs of multiple antenna elements in such a way as to form finely sectionized (directional) beams with more spatial selectivity than it can be achieved with conventional, single element approach.

Adaptive antenna technology represents the most advanced smart antenna approach till date. Using a variety of new intelligent signal-processing algorithms, the adaptive system takes advantage of its ability to effectively locate and track various types of signals to dynamically minimize interference and maximize intended signal reception.

Both of which systems attempts to increase gain according to the location of the user; however, only the adaptive system provides optimal gain while simultaneously identifying, tracking, and minimizing interfering signals. In this thesis adaptive antenna systems are designed and optimized by using the Differential Evolution and Harmony search methods and applying the techniques to the geometries linear array and circular array.

2.2 LINEAR ARRAY

Consider a linear arrangement of N elements which are uniformly distributed separated by a distance d. The array factor can be obtained by considering the elements to be point sources, the total field can be formed by multiplying

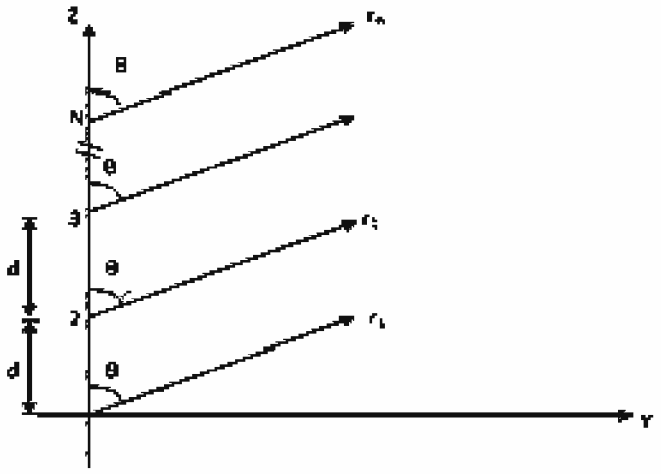

Figure 2.1: Uniform Linear Array

the array factor of the isotropic source by the field of a single element. This is pattern multiplication rule, and is applicable only for arrays consisting of identical elements.

The formulation of the array factor is as follow. The current density value from the far field observation point is given by $J(\xi, \eta, \zeta)$. This current density is a parameter distributed in all three axes as below

$$J(\xi, \eta, \zeta) = J_x(\xi, \eta, \zeta) + J_y(\xi, \eta, \zeta) + J_z(\xi, \eta, \zeta) \tag{2.1}$$

where

$$J_x(\xi, \eta, \zeta) = J_x(x_i + \xi_i, y_i + \eta_i, z_i + \zeta_i)$$

The current density given in Eq.2.1 is radiated for the complex excitation. As the complex excitation changes the current density of the radiator will be varied[22]. Since all the elements are assumed to be identical and similarly oriented, the ratio of current density for the different complex excitations of the radiator follows,

$$\frac{J_x(x_i+\xi_i, y_i+\eta_i, z_i+\zeta_i)}{J_x(x_j+\xi_j, y_j+\eta_j, z_j+\zeta_j)} = \frac{I_i}{I_j} \tag{2.2}$$

With the aid of Eq.2.2 the far field equation with the linear arrangement over a finite volume is given as

$$\begin{aligned} A_\phi(\theta,\phi) = \sum_{i=0}^{N} \int_{V1} [&- \sin\phi J_x(x_i+\xi_i, y_i+\eta_i, z_i+\zeta_i) + \\ &\cos\phi J_x(x_i+\xi_i, y_i+\eta_i, z_i+\zeta_i)] \exp^{jk\iota}, d\xi_i d\eta_i d\zeta_i \end{aligned} \tag{2.3}$$

$$\begin{aligned} A_\theta(\theta,\phi) = \sum_{i=0}^{N} \int_{V1} [&\cos\theta\cos\phi J_x(x_i+\xi_i, y_i+\eta_i, z_i+\zeta_i) + \\ &\cos\theta\sin\phi J_x(x_i+\xi_i, y_i+\eta_i, z_i+\zeta_i)] \exp^{jk\iota}, d\xi_i d\eta_i d\zeta_i \end{aligned} \tag{2.4}$$

Where

$$\iota = \xi\sin\theta\cos\phi + \eta\sin\theta\sin\phi + \cos\theta$$

Considering the distance r_i for the i^th element from the far field observing point then the array factor for a linear field with field as above is

$$A_a(\theta,\phi) = \sum_{n=0}^{N} \frac{I_n}{I_0} \exp^{jkr_n(\cos\alpha\sin\theta\cos\phi + \cos\beta\sin\theta\sin\phi + \cos\gamma\cos\theta)} \tag{2.5}$$

2.3 CIRCULAR ARRAY

Consider a circular arrangement of N elements which are uniformly distributed in circular boundary of radius a as shown in Fig.2.2. The array factor can be obtained by considering the elements to be point source radiation, the total field can be formed by multiplying the array factor of the isotropic source by the field of a single element.

Considering a far field observation point, whose current density distribution in the cartesian coordinate system is given as Eq.2.6

$$K(\xi,\eta,\zeta) = K_x(\xi,\eta,\zeta) + K_y(\xi,\eta,\zeta) + K_z(\xi,\eta,\zeta) \tag{2.6}$$

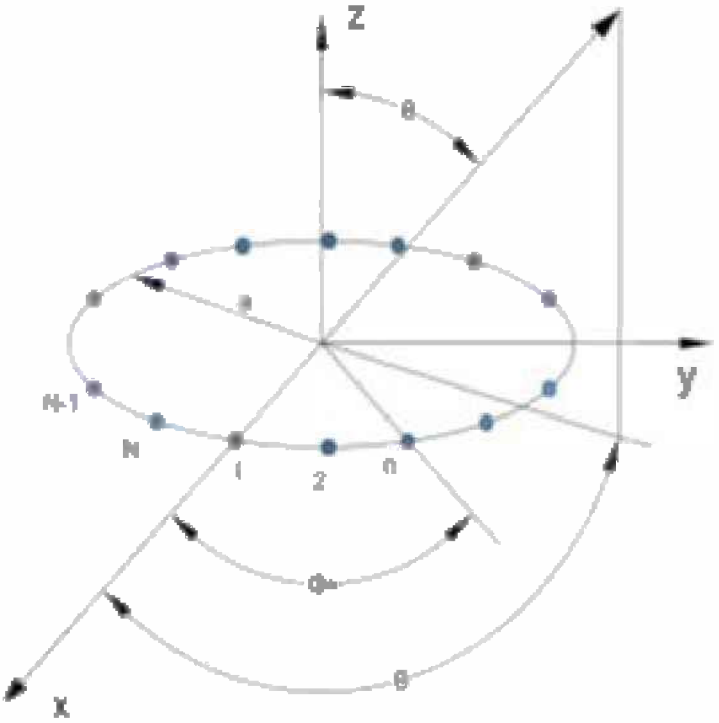

Figure 2.2: Uniform Circular Array

The corresponding E-field of the source elements whose current density $K(\xi, \eta, \zeta)$ is given by

$$A_\theta(\theta, \phi) = \cos\theta \sin\phi \int_S K_y(\xi, \eta) \exp^{jk\iota} d\eta \tag{2.7}$$

$$A_\phi(\theta, \phi) = \cos\phi \int_S K_y(\xi, \eta) \exp^{jk\iota} d\eta \tag{2.8}$$

Where

$$\iota = \xi \sin\theta \cos\phi + \eta \sin\theta \sin\phi + \cos\theta$$

By converting the cartesian coordinate system to the circular coordinate system with consideration as $\xi = \rho\cos\beta$, and $\eta = \rho\sin\beta$. With the circular boundary of aperture a the integral common to eq.2.7 and eq.2.8 can be viewed as the array factor for a linearly polarized planar of aperture distribution

$$F(\theta, \phi) = \int_0^a \int_0^{2\pi} K(\rho, \beta) \exp^{jk\rho \sin\theta \cos(\phi - \beta)} \rho d\rho d\beta \tag{2.9}$$

Applying Fourier series to the aperture distribution and bessel expansion eq.2.6 results

$$K(\rho,\beta) = \sum_{n=-\infty}^{\infty} K_n(\rho)\exp^{jn\beta} \tag{2.10}$$

$$\exp^{jk\rho\sin\theta\cos(\phi-\beta)} = \sum_{m=-\infty}^{\infty} (j)^m J_m(k\rho\sin\theta)\exp^{jm(\phi-\beta)} \tag{2.11}$$

by using the above two expansions on eq.2.9 then the array factor equation is derived as:

$$F(\theta,\phi) = \sum_{m=-\infty}^{\infty}\sum_{n=-\infty}^{\infty}\int_0^a\int_0^{2\pi} K_n(\rho)(j)^m J_m(k\rho\sin\theta)\exp^{jm\phi}\exp^{j(n-m)\beta}\rho d\rho d\beta \tag{2.12}$$

2.4 ADAPTIVE ANTENNA ARRAY MODELING

Linear array modeling

Every element in the array will receive a signal from narrow-band mobile users. Each individual signal is connected through a complex plane consisting of real and imaginary portions assigned to amplitude and phase of the feed. The complex weighting factor is termed as excitation. Here the complex excitation are the linking elements which links signal space with the antenna model. The actual received signal is the correlation of summation of the complex excitation of each element and signal received by the that element. For simplicity mutual coupling is ignored and first element is selected as reference for phase[6].

A uniformly spaced linear array of $N = 5$ isotropic antenna elements spaced a distance $d = \frac{\lambda}{2}$ in the X-axis can be depicted as

$$a(\theta_i) = [1 \;\; \exp^{j\pi\sin\theta_i} \;\; \exp^{j2\pi\sin\theta_i} \;\; \exp^{j3\pi\sin\theta_i} \;\; \exp^{j4\pi\sin\theta_i}] \tag{2.13}$$

The Adaptive linear array is shown in Fig.2.3. The figure itself clears the idea of adaptiveness. Weight estimation block updates the weights depending on the output.

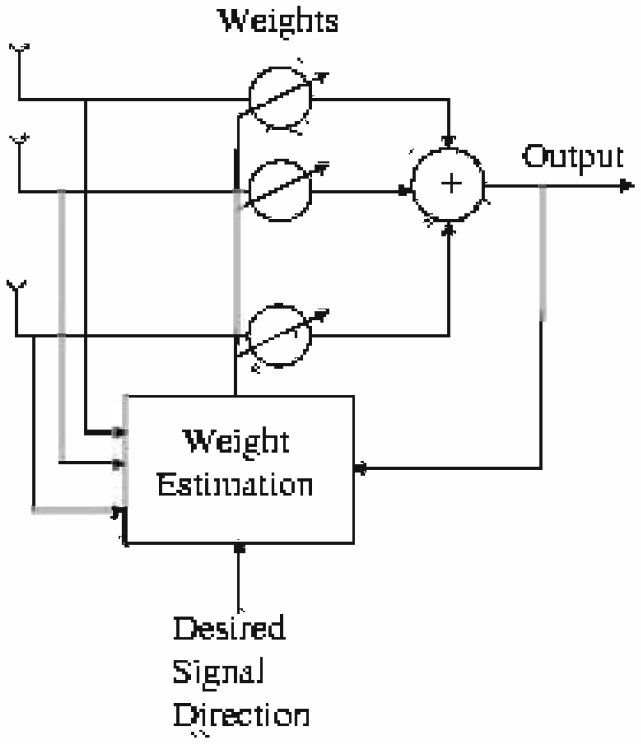

Figure 2.3: Adaptive Linear Array of isotropic elements

Circular array modeling

The Adaptive circular array is shown in Fig.2.4. The figure reveals that the each element in the circular arrangement receives signals and correlation is the product of signal with the corresponding weight of each element. Summation of these individual product signals will be the final signal which will be compared with desired output. Depending on the fitness/cost value which depends on the desired and obtained outputs the value of weights will vary.

A circular array of $N = 5$ elements uniformly spaced on a circle of radius $R = \frac{\lambda}{2}$ the array response vector can be written as

$$a(\theta_i) = \begin{pmatrix} 1 \\ \exp^{-j\pi(\sin(\theta_0))\cos(\phi)-\sin(\theta_i)\cos\phi} \\ \exp^{-j\pi(\sin(\theta_0))\cos(\phi-\frac{2\pi}{5})-\sin(\theta_i)\cos\phi-\frac{2\pi}{5}} \\ \exp^{-j\pi(\sin(\theta_0))\cos(\phi-\frac{4\pi}{5})-\sin(\theta_i)\cos\phi-\frac{4\pi}{5}} \\ \exp^{-j\pi(\sin(\theta_0))\cos(\phi-\frac{6\pi}{5})-\sin(\theta_i)\cos\phi-\frac{6\pi}{5}} \\ \exp^{-j\pi(\sin(\theta_0))\cos(\phi-\frac{8\pi}{5})-\sin(\theta_i)\cos\phi-\frac{8\pi}{5}} \end{pmatrix}$$

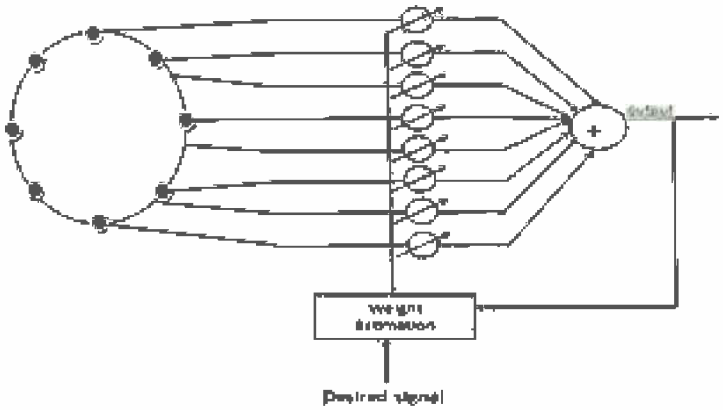

Figure 2.4: Adaptive Linear Array of isotropic elements

Where θ_0 = elevation angle and it is fixed at $\frac{\pi}{4}$
ϕ = azimuthal angle and it is fixed at 0^0
And $X = VS + VI, X$ = received signal vector

Chapter 3

SMART ANTENNA SYNTHESIS USING DE HS and IHS

3.1 DIFFERENTIAL EVOLUTION

Evolutionary algorithms (EAs) are population-based stochastic algorithms that can effectively handle real-world optimization problems which are non-continuous and/or non-differentiable and characterized by chaotic disturbances, randomness and complex nonlinear dynamics. DE is a Stochastic Direct Search and Global Optimization algorithm. It uses rather greedy selection and less stochastic approach to solve optimization problems when compared to other classical EAs. DE is an evolutionary computation method that was originally introduced by Storn and Price in 1995. Furthermore, it has been modified by researchers to be a reliable and versatile function optimizer that is also readily applicable to a wide range of optimization problems. Mutation and Crossover strategies along with their associated parameters shows the effectiveness of the conventional DE in solving numerical optimization problems. DE has the ability to find the global minimum regardless of the initial parameter values and can give reasonably fast convergence.
DE uses a population of size P, composed of floating point encoded individuals that evolve over generations G to reach an optimal solution. Each Wo is a vector that contains as many parameters as the problem decision vari-

Input Parameters $W = \begin{pmatrix} w_{1,1} & \cdots & w_{1,N} \\ \vdots & \ddots & \vdots \\ w_{P,1} & \cdots & w_{P,N} \end{pmatrix}$, F, CR, P=population value

Output parameter w_o

Evaluate fitness $F = fitness(W)$, $F = [\ f_1 \quad \ldots \quad f_H MS\ ]$

For iter < itermax

|

|

| MUTATION

| |

| | $W_1 = W(a,:) + F(W(b,:) - W(c,:))$, $a, b, c =$ any random integers

| |

| CROSS OVER

| | $W_n = \begin{cases} W_1 & rand \leq CR \\ W & otherwise \end{cases}$

| |

0 | Evaluate fitness $F_n = fitness(W_n)$, $F = [\ f_1 \quad \ldots \quad f_p\ ]$

| $W_o = \begin{cases} W_n & F_n < F \\ W & otherwise \end{cases}$

end

Table 3.1: DE PSEUDO Code

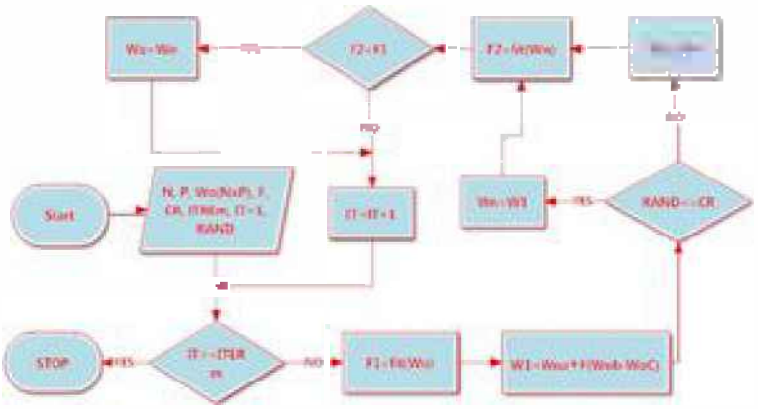

Figure 3.1: DE flow chart

ables D. The population size P is an algorithm control parameter selected by the user which remains constant throughout the optimization process. With the present weight present fitness is found and compared with the new fitness value the weights will be updated by employing mutation and crossover. PSEUDO code of the algorithm prsented in table.3.1.

The update equations followed with a flowchart, explaining the DE tech-

Parameter	Description
N	Number of Users
P	Population ($50 or 100$)
F	Scaling Factor ($0 to 2$
CR	Crossover constant ($0 to 1$)
$ITERm$	Maximum Iterations
IT	Current iteration value
$RAND$	Random Variable Matrix
W_o	Weight Matrix
W_n	New Weight Matrix
F_1 and F_2	Old and New Fitness values

Table 3.2: DE Parameter description

nique is shown in the Fig.3.1 And each parameters description is given in the table.3.2.

3.1.1 SIMULATION RESULTS

Considering the linear array geometry the simulation results for multi users and multi interferences are follows by employing DE.

Simulation.I

Simulation is conducted by taking a single interference initially with 5 users and result is as shown in Fig.3.2. DOA is considered at 60^0 and interference is at 30^0.

Simulation.II

Simulation of the linear array is continued by increasing the number of interference to two and are at $[30^0, 90^0]$. The synthesized radiation pattern of adaptive antenna array is as shown in fig.3.3.

Simulation.III

Now the simulation repeated for 5 users with AOA at 60^0, considering three interferences at $[-30^0, -60^0, 30^0]$. The field pattern of the adaptive antenna array with the above considerations is shown in Fig.3.4.

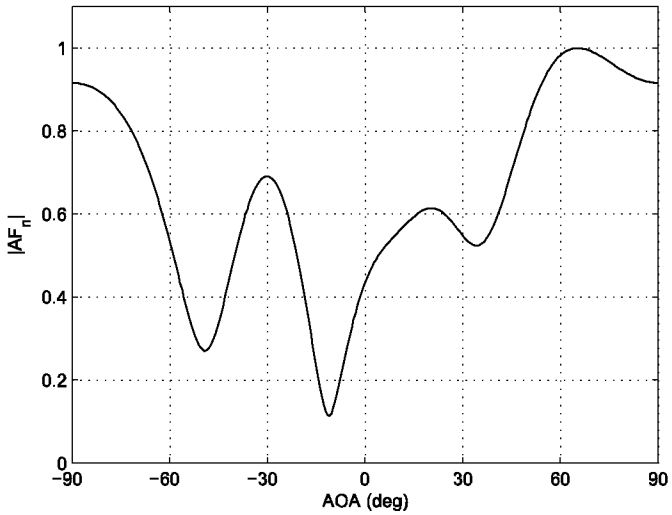

Figure 3.2: Intensity level plot with one interference for 5 users

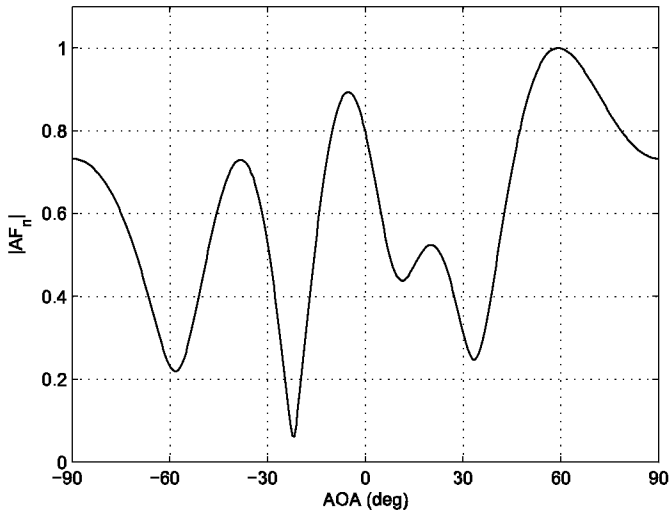

Figure 3.3: Intensity level plot with two interferences for 5 users

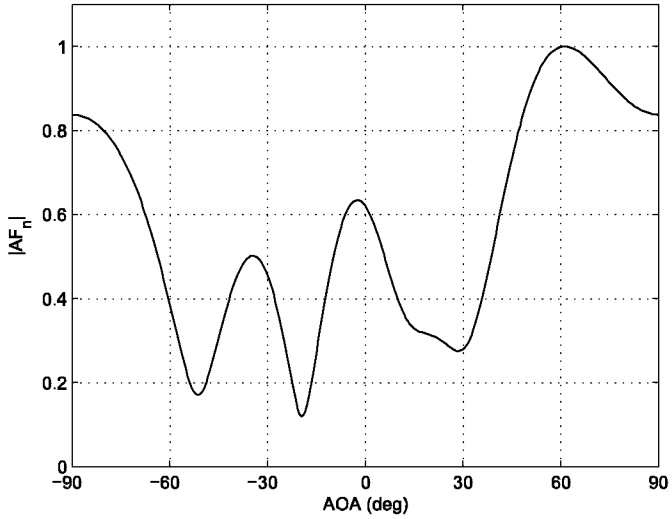

Figure 3.4: Intensity level plot with three interferences for 5 users

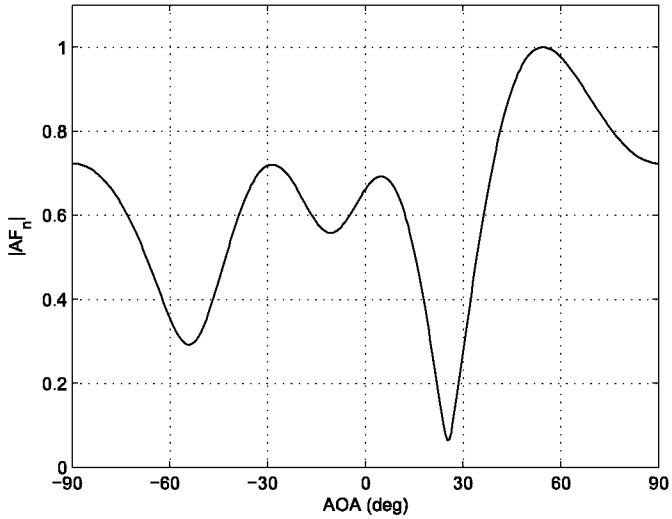

Figure 3.5: Intensity level plot with four interferences for 5 users

Simulation.IV

Now the number of interferences are increased to 4 for 5 users. AOA is considered at 60^0 and interference levels are considered at $[-30^0, -60^0, 30^0, 90^0]$. The radiation pattern of the antenna array with above considerations is shown in Fig.3.5.

Simulation.V

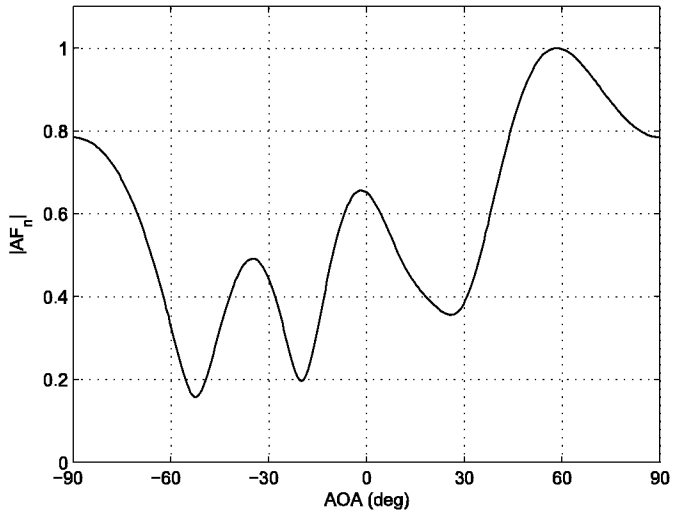

Figure 3.6: Intensity level plot with five interferences for 5 users

For the same number of users the interference level is increased by another one level i.e. in this case interferences considered are 5 and are at $[-30^0, -60^0, 30^0, 90^0, 10^0]$. And AOA is considered at 60^0. The radiation field pattern for the above consideration is as shown in Fig.3.6.

Simulation.VI

Simulation is conducted by taking a single interference initially with 10 users and result is as shown in Fig.3.7. DOA is considered at 60^0 and interference is at 30^0.

Simulation.VII

For the same number of users the interference level is considered at 60^0 and AOA is considered at 10^0. The radiation field pattern for the above consideration is as shown in Fig.3.8.

Simulation.VIII

Simulation of the linear array is continued by increasing the number of in-

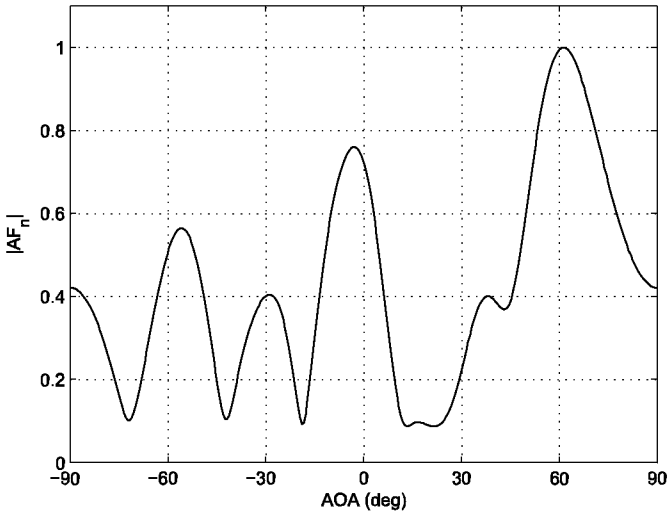

Figure 3.7: Intensity level plot with one interference for 10 users

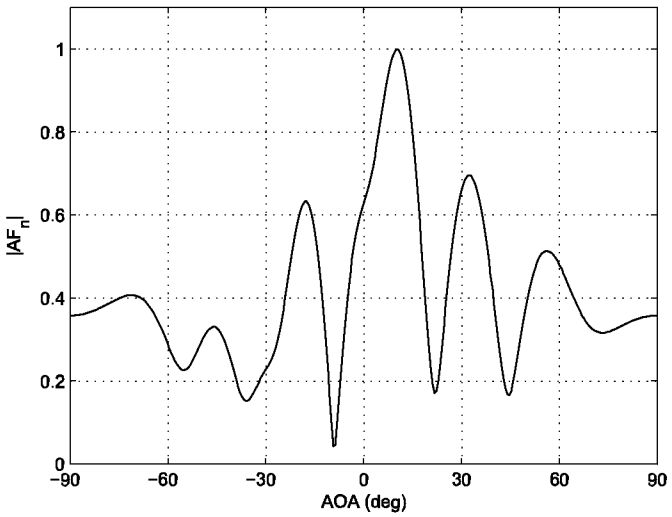

Figure 3.8: Intensity level plot for 10 users

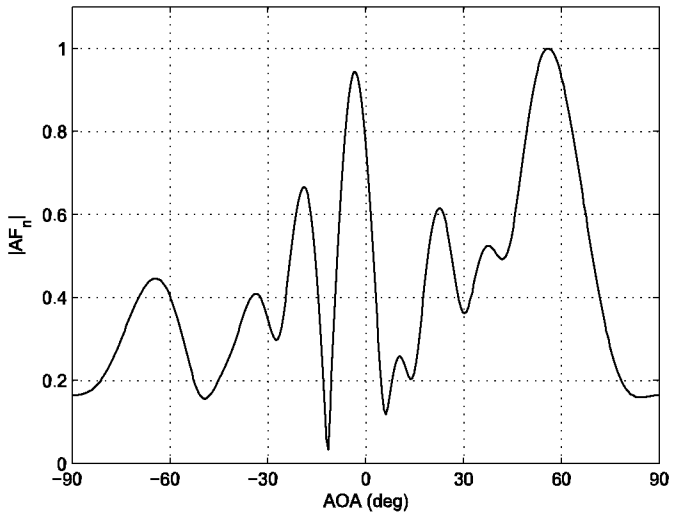

Figure 3.9: Intensity level plot with two interferences for 10 users

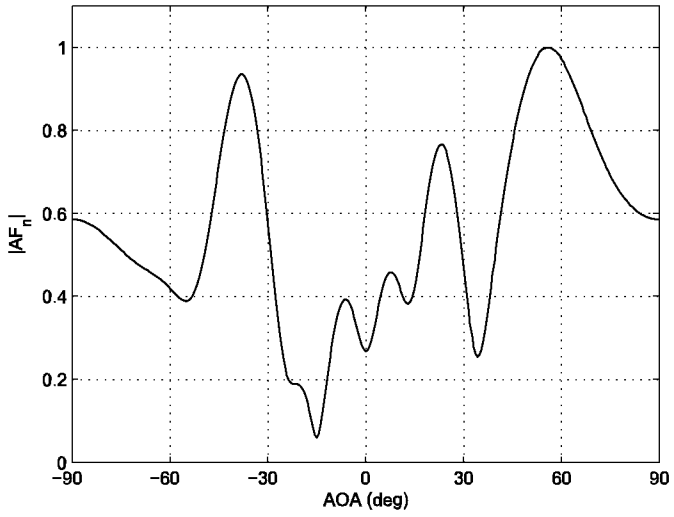

Figure 3.10: Intensity level plot with three interferences for 10 users

terference to two and are at $[30^0, 90^0]$. The synthesized radiation pattern of adaptive antenna array is as shown in fig.3.9.

Simulation.IX

Now the simulation repeated for 10 users with AOA at 60^0, considering three interferences at $[-30^0, -60^0, 30^0]$. The field pattern of the adaptive antenna array with the above considerations is shown in Fig.3.10.

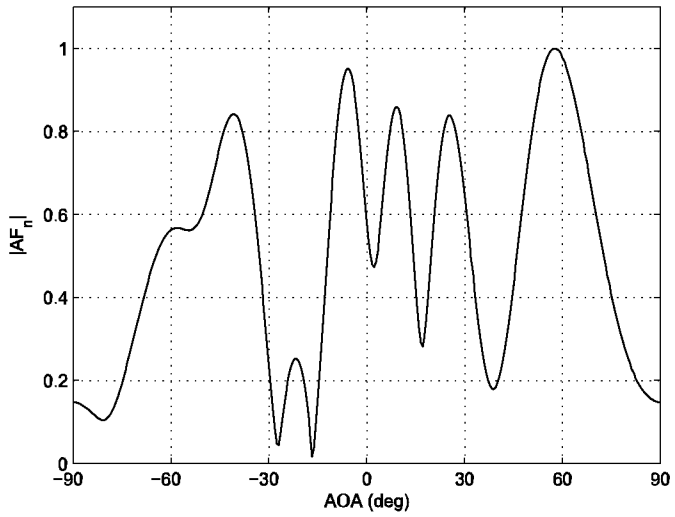

Figure 3.11: Intensity level plot with four interferences for 10 users

Simulation.X

Now the number of interferences are increased to 4 for 5 users. AOA is considered at 60^0 and interference levels are considered at $[90^0, -30^0, -60^0, 10^0,]$. The radiation pattern of the antenna array with above considerations is shown in Fig.3.11.

Simulation.XI

For the same number of users the interference level is increased by another one level i.e. in this case interferences considered are 5 and are at $[90^0, 30^0, -30^0, -60^0, 90^0]$. And AOA is considered at 60^0. The radiation field pattern for the above consideration is as shown in Fig.3.12.

Now the simulation is extended to the other geometry which is circular arrangement of the elements. The simulated results for the different cases are shown below.

Simulation I

Simulation is conducted by taking a single interference initially with 5 users

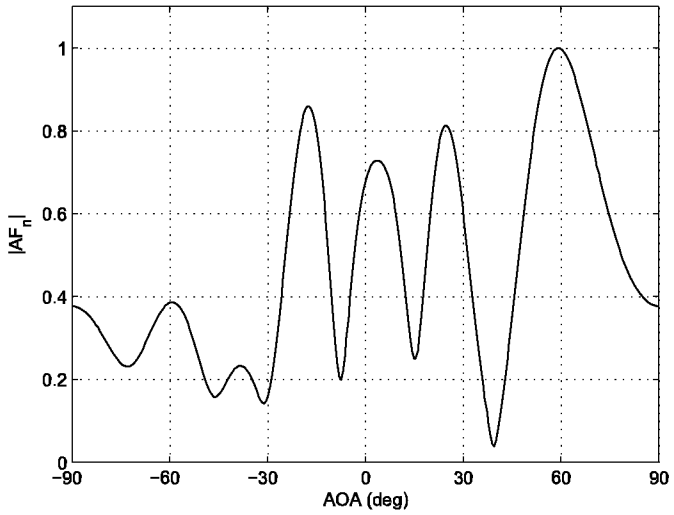

Figure 3.12: Intensity level plot with five interferences for 10 users

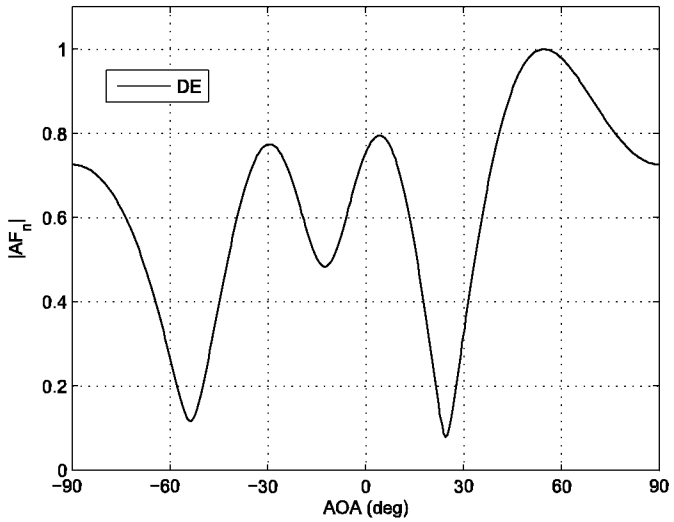

Figure 3.13: Intensity level plot with one interference for 10 users

and result is as shown in Fig.3.13. DOA is considered at 60^0 and interference is at 30^0.

Simulation.II

For the same number of users the interference level is increased to 5 and are at $[-30^0, -60^0, 30^0, 90^0, 10^0]$. And AOA is considered at 60^0. The radiation field pattern for the above consideration is as shown in Fig.3.14.

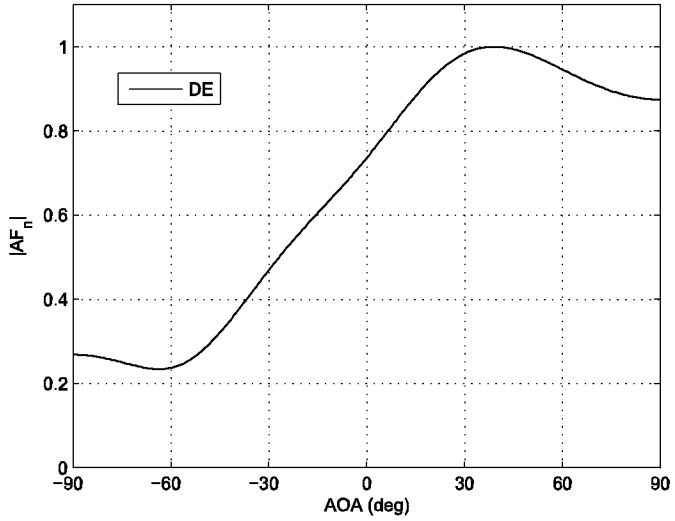

Figure 3.14: Intensity level plot with five interferences for 5 users

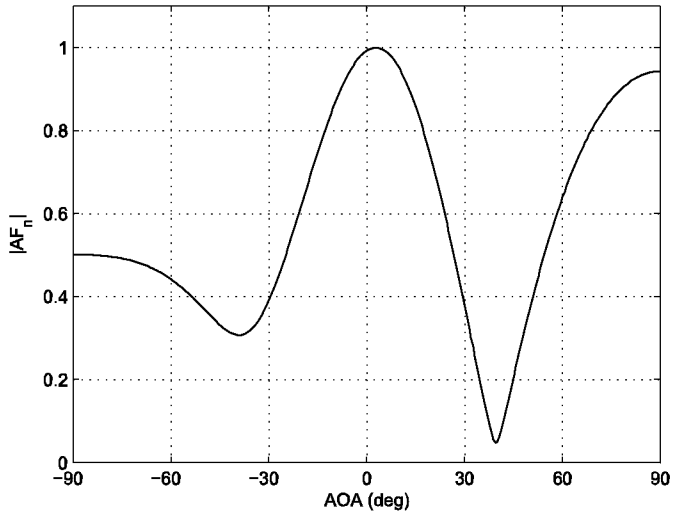

Figure 3.15: Intensity level plot for 10 users

Simulation.III

For the same number of users the interference level is considered at 60^0 and AOA is considered at 10^0. The radiation field pattern for the above consideration is as shown in Fig.3.15.

From the above simulation results it is observed that DE performs well for linear geometry. For the linear geometry the AOA detection is impressive and AOI detection in satisfied level but for circular geometry the beam width at the AOA is more and intensity level at AOI is not a null. Even the interference level in linear geometry at AOI is also not a null but comparatively in satisfied with circular geometry.

3.2 HARMONY SEARCH

The HS is a met-heuristic algorithm which is inspired from the improvisation of a musician. Initially developed by Zong woo geem in 2000. Specifically the process by which the musicians rapidly refine their individual improvisation through variation resulting in an aesthetic harmony even if they have never played together [6]. Here in our application each users treated as a musician and each instruments pitch and range corresponds to the bounds and constraints on the decision variable. The harmony between the musicians is taken as results when the audience aesthetic appreciation which is considered as cost function is in desired level. Every time musicians seek harmony over time through small variation to get the best cost[23]. Current meta-heuristic algorithms imitate natural phenomena, i.e., physical annealing in simulated annealing, human memory in tabu search, and evolution in evolutionary algorithms. HS meta-heuristic algorithm was conceptualized using the musical process of searching for a perfect state of harmony. Musical performances seek to find pleasing harmony (a perfect state) as determined by an aesthetic standard, just as the optimization process seeks to find a global solution (a perfect state) as determined by an objective function. The pitch of each musical instrument determines the aesthetic quality, just as the objective function value is determined by the set of values assigned to each decision variable. The new HS meta-heuristic algorithm was derived based on natural musical performance processes that occur when a musician searches for a better state

Input Parameters $W = \begin{pmatrix} w_{1,1} & \cdots & w_{1,HMS} \\ \vdots & \ddots & \vdots \\ w_{N,1} & \cdots & w_{N,HMS} \end{pmatrix}$, HMS, PAR, HMCR
Output parameter w_o
Evaluate fitness $F = fitness(W)$, $F = [\ f_1 \quad \ldots \quad f_{HMS}\ ]$
For iter < itermax
|
| if rand() < HMCR
| | W_n = rand(:,HMS)
| else
| | $W_n = W(:,i)$, i=any random integer
| end
| | if rand() < PAR
| | $W_n = W_n + BW$
| | BW = generally range of adjustment
| else
| | $W_n = W_n$+ random pitch
| end
| Evaluate fitness $F_n = fitness(W_n)$, $F = [\ f_1 \quad \ldots \quad f_HMS\ ]$
| $W_o = \begin{cases} W_n & F_n < F \\ W & otherwise \end{cases}$
end

Table 3.3: HS PSEUDO Code

of harmony, such as during jazz improvisation.When a musician improvises one pitch, usually he (or she) follows any one of three rules: (1) playing any one pitch from his (or her) memory, (2) playing an adjacent pitch of one pitch from his (or her) memory, and (3) playing totally random pitch from the possible sound range. Similarly, when each decision variable chooses one value in the HS algorithm, it follows any one of three rules: (1) choosing any one value from the HS memory (defined as memory considerations), (2) choosing an adjacent value of one value from the HS memory (defined as pitch adjustments), and (3) choosing totally random value from the possible value range (defined as randomization)[18]. The three rules in HS algorithm are effectively directed using two parameters, i.e., harmony memory considering rate (HMCR) and pitch adjusting rate (PAR). Algorithm PSEUDO code is provided in table.3.3.

The update equations followed with a flowchart, explaining the DE tech-

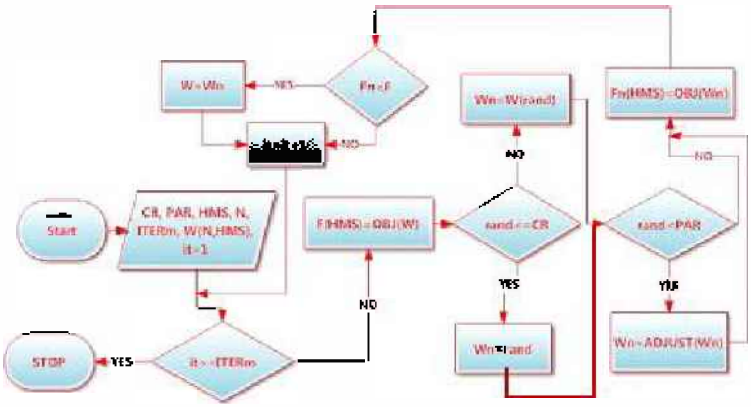

Figure 3.16: HS flow chart

Parameter	Description
N	Number of Users
HMS	Harmony Memory Size ($50 or 100$)
CR	Considering Rate ($0.77 to 0.99$)
PAR	Pitch Adjusting Rate ($0.1 to 0.5$)
$ITERm$	Maximum Iterations
IT	Current iteration value
$RAND$	Random Variable Matrix
W	Weight Matrix
W_n	New Weight Matrix
F	Fitness values
F_n	New Fitness Value

Table 3.4: HS Parameter description

nique is shown in the Fig.3.16 And each parameters description is given in the table.3.4.

3.2.1 SIMULATION RESULTS

Considering the linear array geometry the simulation results for multi users and multi interferences are follows by employing HS.

Simulation.I

Simulation is conducted by taking a single interference initially with 5 users and result is as shown in Fig.3.17. DOA is considered at 30^0 and interference is at 60^0.

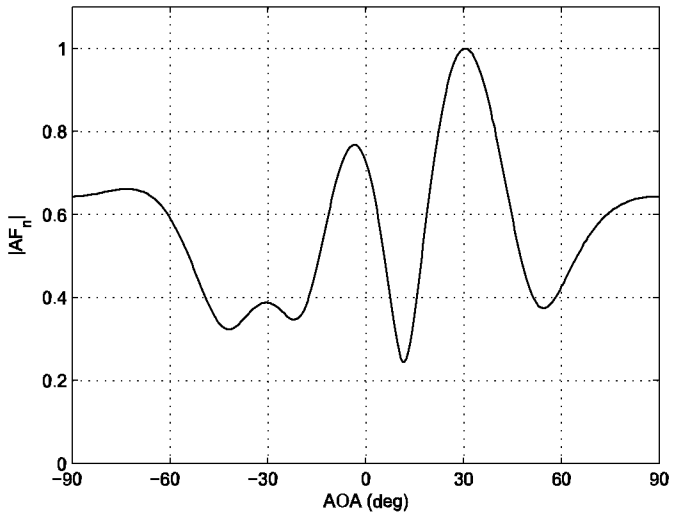

Figure 3.17: Intensity level plot with one interference for 5 users by HS

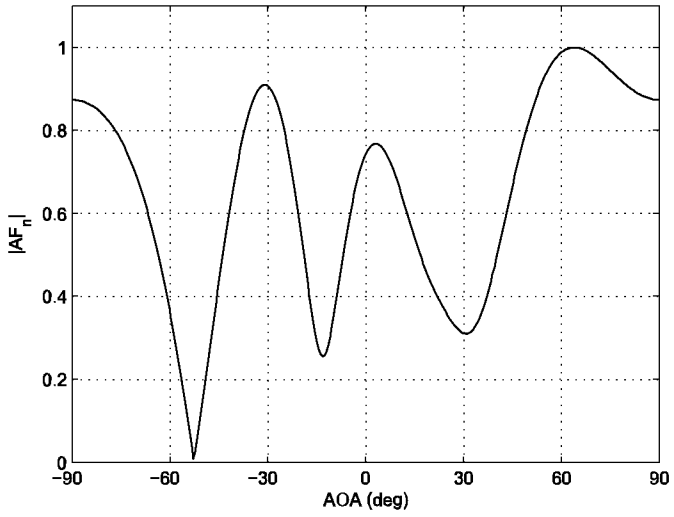

Figure 3.18: Intensity level plot with two interferences for 5 users by HS

Simulation.II

Simulation of the linear array is continued by increasing the number of interference to two and are at $[30^0, 90^0]$. The synthesized radiation pattern of adaptive antenna array is as shown in fig.3.18. For 5 users with considering AOA at 60^0.

Simulation.III

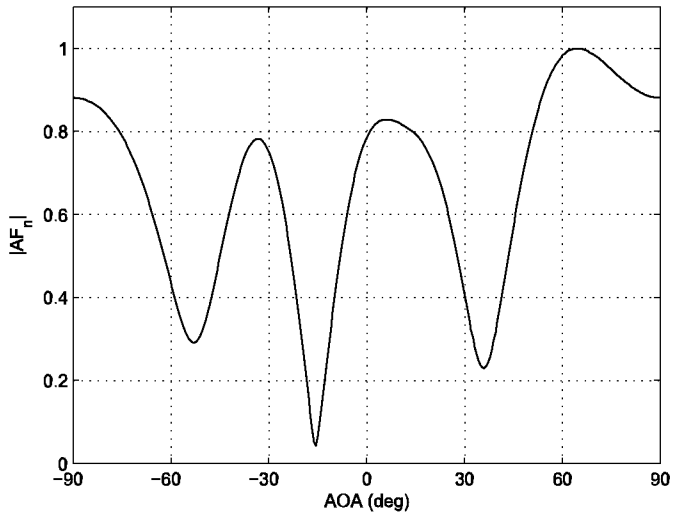

Figure 3.19: Intensity level plot with three interferences for 5 users by HS

Now the simulation repeated for 5 users with AOA at 60^0, considering three interferences at $[-30^0, -60^0, 30^0]$. The field pattern of the adaptive antenna array with the above considerations is shown in Fig.3.19.

Simulation.IV

For the same number of users the interference level is increased by another two level i.e. in this case interferences considered are 5 and are at $[-30^0, -60^0, 30^0, 90^0, 10^0]$. And AOA is considered at 60^0. The radiation field pattern for the above consideration is as shown in Fig.3.20.

Simulation.V

Simulation is conducted by taking a single interference with 5 users and result is as shown in Fig.3.21. DOA is considered at 10^0 and interference is at 60^0.

Simulation.VI

Simulation is conducted by taking a single interference initially with 10 users and result is as shown in Fig.3.22. DOA is considered at 10^0 and interference is at 60^0.

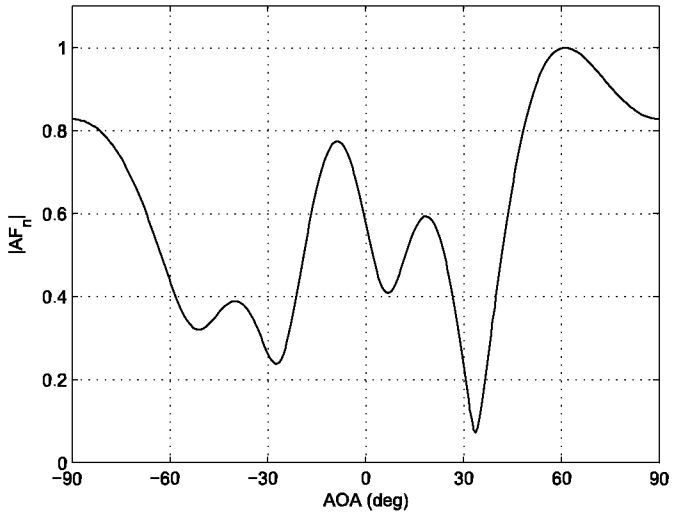

Figure 3.20: Intensity level plot with five interferences for 5 users by HS

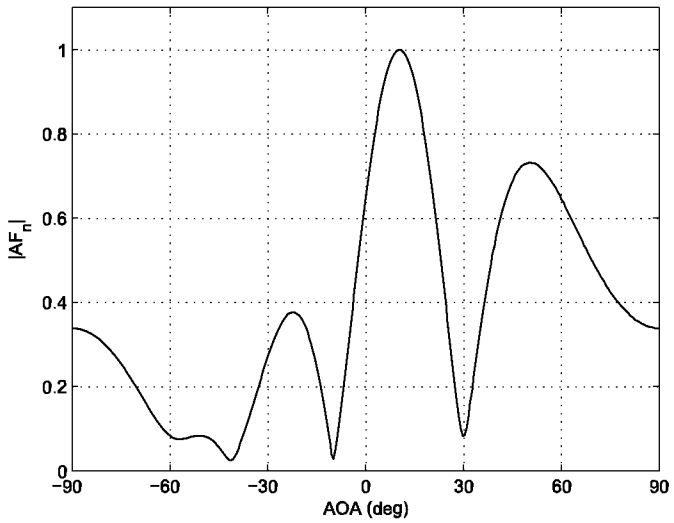

Figure 3.21: Intensity level plot with one interferences for 5 users by HS

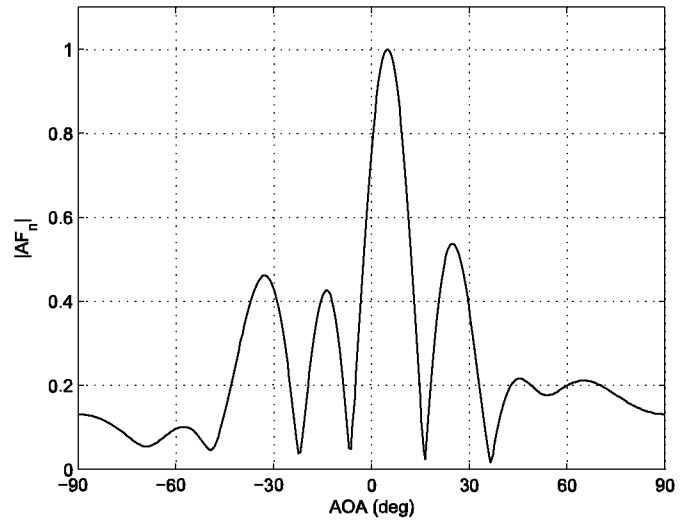

Figure 3.22: Intensity level plot with one interference for 10 users by HS

Now the simulation is extended to the other geometry which is circular arrangement of the elements. The simulated results for the different cases are shown below.

Simulation I

Simulation is conducted by taking a single interference initially with 5 users and result is as shown in Fig.3.23. DOA is considered at 30^0 and interference is at 60^0.

Simulation.II

Simulation is conducted by taking a single interference with 5 users and result is as shown in Fig.3.24. DOA is considered at 10^0 and interference is at 60^0.

Simulation.III

Simulation is conducted by taking a single interference initially with 10 users and result is as shown in Fig.3.25. DOA is considered at 10^0 and interference is at 60^0.

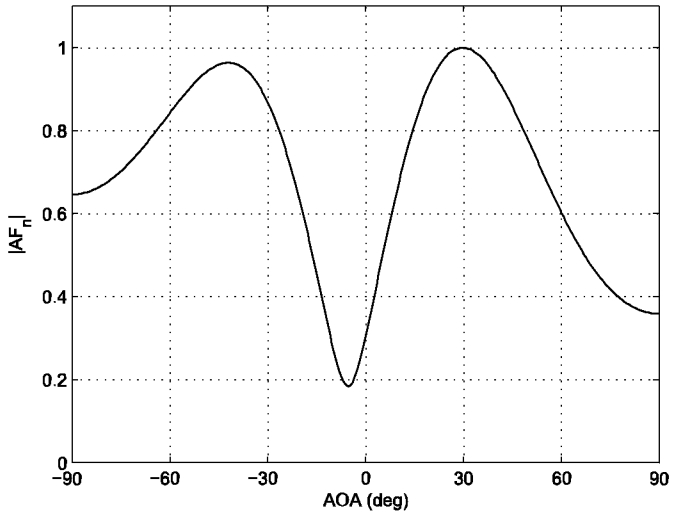

Figure 3.23: Intensity level plot with one interference for 5 users for circular array

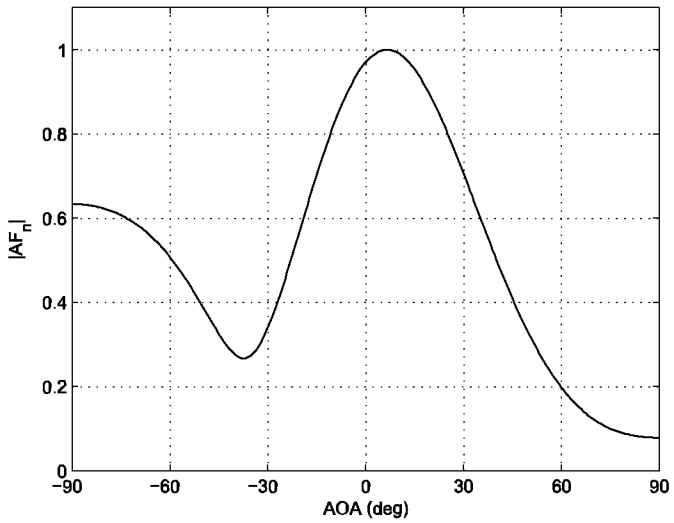

Figure 3.24: Intensity level plot with one interferences for 5 users by HS

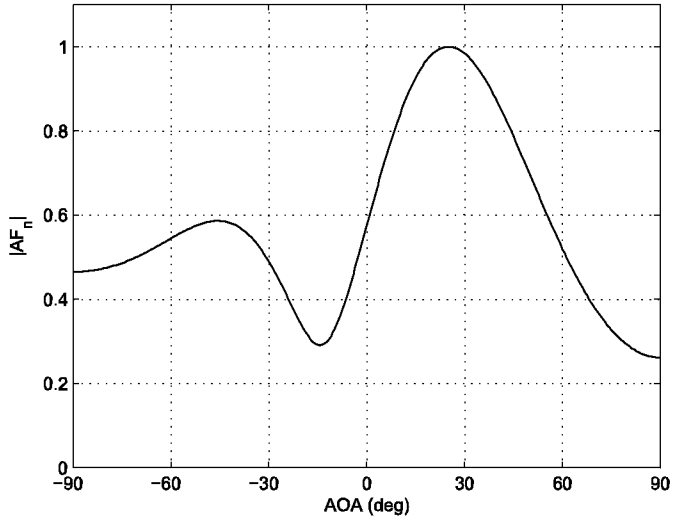

Figure 3.25: Intensity level plot with one interference for 10 users by HS

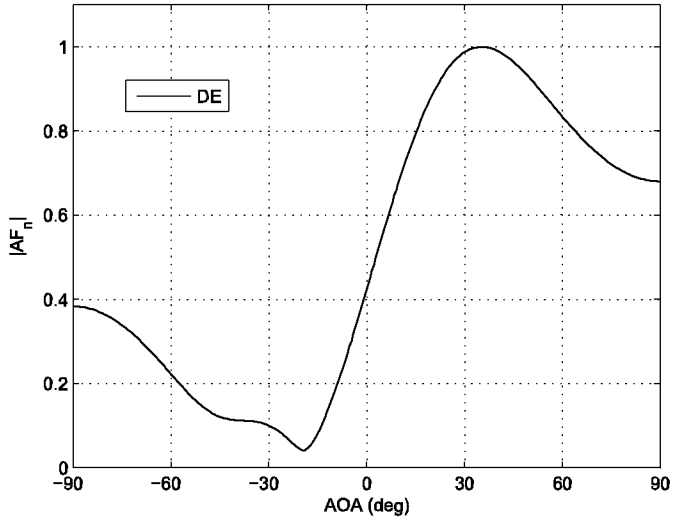

Figure 3.26: Intensity level plot with two interferences for 10 users

Simulation.IV

Simulation of the linear array is continued by increasing the number of interference to two and are at $[30^0, 90^0]$. The synthesized radiation pattern of adaptive antenna array is as shown in fig.3.26.

Simulation.V

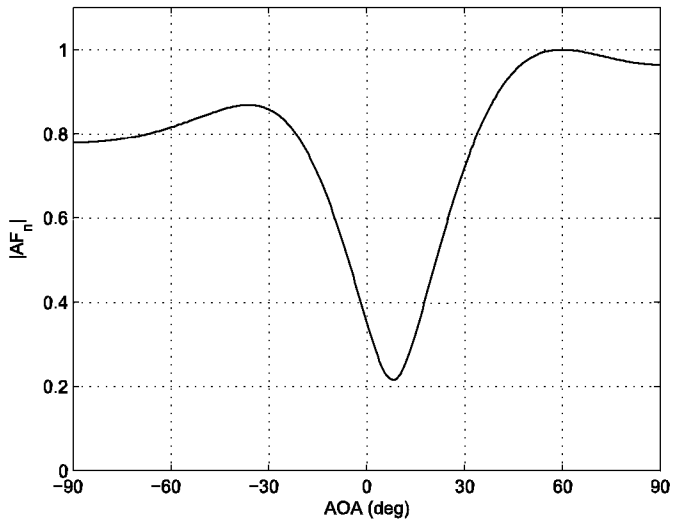

Figure 3.27: Intensity level plot with five interferences for 5 users

For the same number of users the interference level is increased by another one level i.e. in this case interferences considered are 5 and are at $[-30^0, -60^0, 30^0, 90^0, 10^0]$. And AOA is considered at 60^0. The radiation field pattern for the above consideration is as shown in Fig.3.27.

3.3 COMPARISON OF DE AND HS

In this section the discussion is about the comparison between the two evolutionary techniques DE and HS. This comparison is made for the two types of geometrical arrangement those are linear element arrangement and circular element arrangement. In the below discussion initial four simulations are for linear arrangement of the elements, and the remaining 2 simulation are for the circular arrangement of the elements.

Simulation.I

Simulation of the linear array is continued by increasing the number of interference to two and are at $[30^0, 90^0]$. The synthesized radiation pattern of adaptive antenna array is as shown in fig.3.28. For 5 users with considering

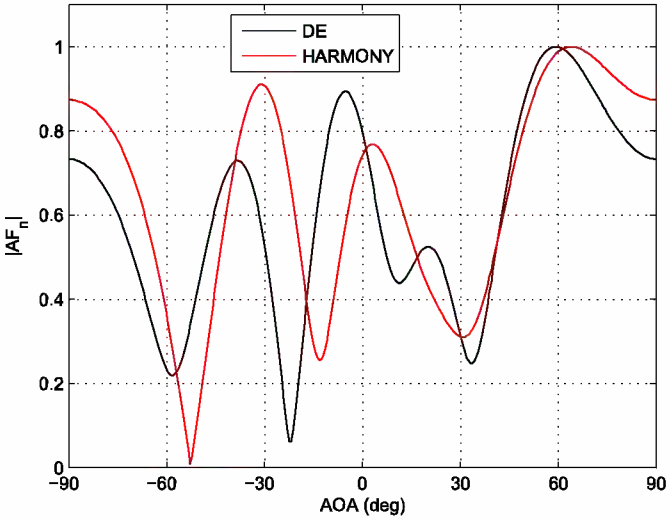

Figure 3.28: Comparison of DE and HS with 1 interference with 5 users

AOA at 60^0.

The graphical analysis clears that DE outperforms HS in the accurate detection of the main beam. The polar plot analysis clearly gives that the radiation intensity level at the interference angle is not reduced to a minimum value using the HS technique.

Simulation.II

Now the simulation repeated for 5 users with AOA at 60^0, considering three interferences at $[-30^0, -60^0, 30^0]$. The field pattern of the adaptive antenna array with the above considerations is shown in Fig.3.29.

Fig.3.29 gives the stability of DE in detecting the AOA and AOI which are the main objectives.However in HS technique accuracy in detection is not maintained.

Simulation.III

For the same number of users the interference level is increased by another two level i.e. in this case interferences considered are 5 and are at $[-30^0, -60^0, 30^0, 90^0, 10^0]$. And AOA is considered at 60^0. The radiation field pattern for the above consideration is as shown in Fig.3.30.

Fig3.30 shows the fact that with a rapid increase in the interferences HS

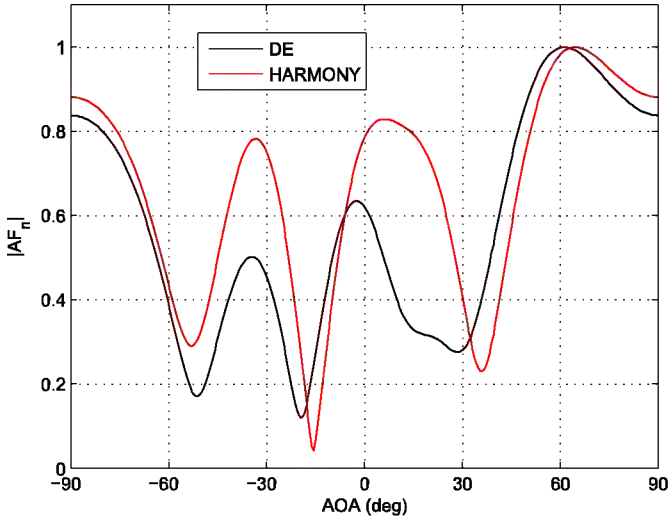

Figure 3.29: Comparison of DE and HS with 3 interference with 5 users

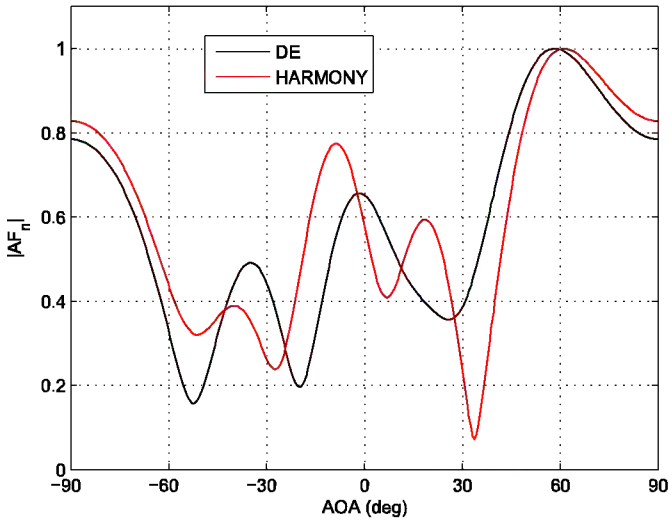

Figure 3.30: Comparison of DE and HS with 5 interference with 5 users

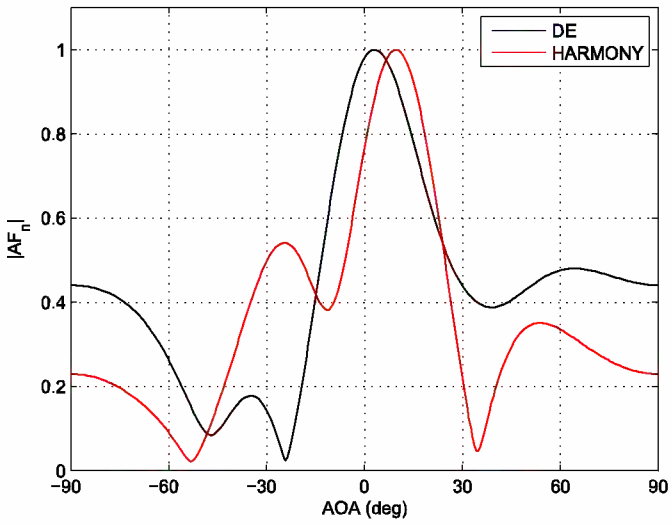

Figure 3.31: Comparison of DE and HS with 1 interference with 10 users

and DE is not consistent in accurately detecting all the interferences. But the AOA detection objective is satisfied by both the techniques.

Simulation.IV

Performance comparison of both the algorithms for 10^0 numbers of users and considering one-interference at 60^0 and AOA at 10^0 is done. HS technique adapts for one objective (AOI) and DE for the other (AOA). From the extensive simulation study on the linear geometry arrangement the overall objective function with a little trade off can be satisfied by DE. In computational time and parametric set up point of view also DE outperforms HS.

Simulation.V

Simulation is continued for circular array by increasing the number of users to 10 and decreasing the number of interferences from 10 to 1. AOA is 10^0 and AOI is 60^0.

The graphical analysis of the field pattern in the Fig.3.32 concludes a circular arrangement though optimized with powerful evolutionary tools does not meet the multiple objectives. It gives an insight of wider beam coverage.

Simulation.VI

Continuation of the simulation further to the circular array and comparing

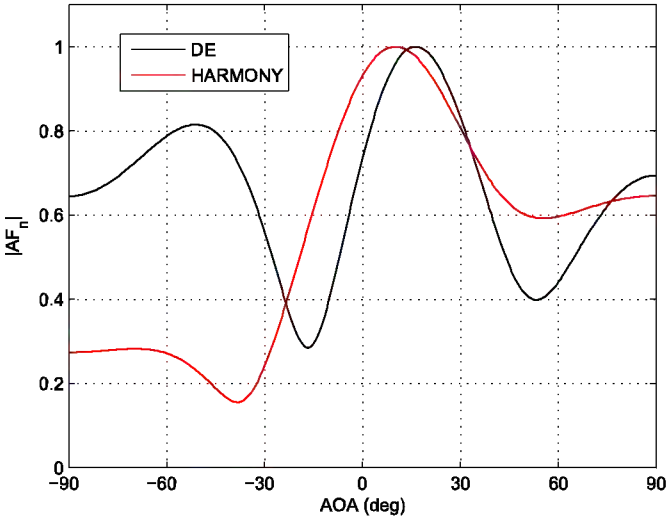

Figure 3.32: Comparison of DE and HS with 1 interference with 10 users

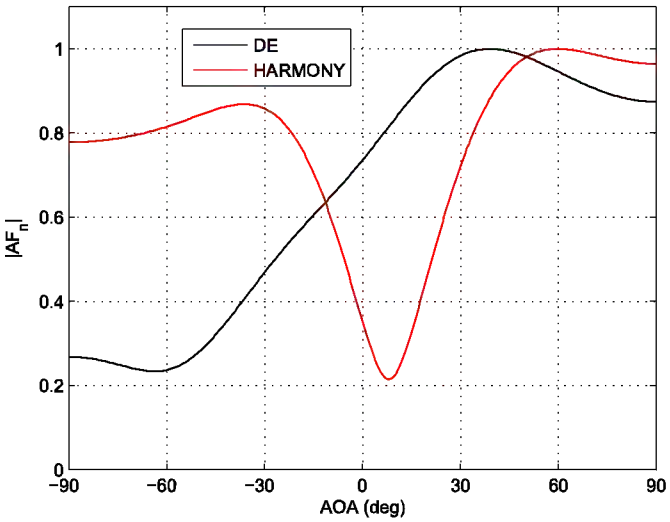

Figure 3.33: Comparison of DE and HS with 5 interference with 5 users

the both algorithms is taken up. Five number of users with AOA at 60^0 and the number of interferences are 5 and are at $[-30^0, -60^0, 30^0, 90^0, 10^0]$. The radiation pattern of both techniques are shown in Fig3.33.

The field pattern in the Fig3.33 conveys that the circular arrangement though optimized using DE and HS couldn't meet the desired/both objectives.

The complex excitation weights for the linear and circular geometry by em-

USERS	AOA(in^0)	AOI(in^0)	OPTIMIZED COMPLEX EXCITATIONS(HS)	OPTIMIZED COMPLEX EXCITATION (DE)
5	60	30, 90	[-0.3464+0.6024i 1+0i 0.3214+0.5934i -0.3719-0.1546i -0.0494+0.7904i]	[1+0i 0.2724-0.1522i 0.5384-0.2211i 0.1962+0.6326i 0.0233-0.9319i]
5	60	-30, -60,30	[1+0i 0.1747+0.4309i 0.0364+0.0188i 0.0063+0.9043i 0.2688-0.3530i]	[0.2325+0.5273i 0.3951-i0.7437i 0.2721+0.3401 -0.1121-0.5469i 1+0i]
5	60	-30, -60,30,90,10	[-0.2057+0.7795i -0.0556-0.6237i 0.4330+0.6120i 0.4750-0.2956i 1+0i]	[-0.6069+0.3566i 1+0i 0.0954+0.9220i 0.1101-0.0651i 0.1818+0.6304i]
10	10	60	[-0.0171-0.3237i 0.0856-0.8662i 0.0029-0.4531i 0.2309-0.2012i 0.5153+0.2222i 0.0709+0.4881i 0.3072-0.2445i 0.2523-0.0879i 1+0i 0.2218+0.2871i]	[0.3414+0.1369i 0.2501-0.3946i 1+0i 0.4322+0.2662i 0.3423+0.0971i -0.3702+0.4990i 0.4408+0.7204i - 0.1111+0.6486i -0.3217-0.1249i 0.2672-0.7371i]

Table 3.5: Optimized complex weights for linear arrangement with different scenarios

USERS	AOA(in^0)	AOI(in^0)	OPTIMIZED COMPLEX EXCITATIONS(HS)	OPTIMIZED COMPLEX EXCITATION (DE)
5	60	[-30,-60, 30,90,10]	[0.1198- 0.2270i 1+0i 0.2552-0.4956i - 0.0462-0.9075i -0.3656-0.3033i]	[1+0i 0.3092+0.0926i 0.0079+0.7740i 0.0577-0.7527i 0.2418+0.0337i]
10	10	60	[-0.2123-0.9212i 0.1462-0.6589i 0.0736+0.3687i 0.0339+0.0324i 0.0873-0.0951i 0.4333+0.2128i -0.2225-0.1723i 0.3736-0.3490-0.3007i 0.3375-0.1717i]	[-0.0546+0.8508i 0.1039+0.3865i - 0.1042-0.1177i -0.4186-0.4057i 0.3051+0.0552i -0.2225-0.1723i 0.3736-0.7792i 1+0i 0.0852 +0.3424i -0.5682-0.0530i]

Table 3.6: Optimized complex weights for the circular geometry for different scenarios

ploying two techniques are tabled below in table (3.5),(3.6).

Both the adaptive techniques performance measurement in achieving 0db at the angle of inference failed. On a comparative analysis the radiation

	users	AOA(in^0)	AOI(in^0)	DE ($indB$)	HS ($indB$)
LINEAR	5	60	30	0.5	0.65
	5	60	30,90	0.3, 0.7	0.3, 0.9
	5	60	-30, -60, 30	0.45, 0.4, 0.3	0.78, 0.4, 0.4
	5	60	-30, -60, 30, 90, 10	0.42, 0.3, 0.4 0.8, 0.55	0.25, 0.4, 0.2, 0.85, 0.75
	10	10	60	0.5	0.2
CIRCULAR	5	30	60	0.85	0.5
	5	60	-30, -60, 30, 90, 10	0.5, 0.25, 0.9, 0.85, 0.8	0.9, 0.8, 0.7, 0.9, 0.2
	10	10	60	0.45	0.6
	10	60	30, 90	0.2, 0.85	0.9, 0.7

Table 3.7: Representation of intensity level at the interferences

spilled over at the inference angle/angles for multi users has been analyzed. The statistical table comprises the percentage of radiated power at the interference angles. Lower the power better is the performance.

3.4 IMPROVED HARMONY SEARCH

As discussed in sec.3.2 two parameters which dictates most impact on the performance of algorithm are HMCR and PAR. These two parameters are involved with the mutation and crossover by which new weights are conceived. Tuning of these two parameters to an accurate value is very important to obtain the optimal solution[19].These parameters are introduced to allow the solution escape from local optima and reach/drive towards the global optimum prediction of the HS algorithm[16]. Initially the values of HMCR and PAR are considered with in the range. This selection of parameters is purely random. That is a value in the range is selected for the optimization blindly whether it leads to optimal solution or not. One of the suitable solution for this problem is adapting the values of the controlling parameters which are HMCR and PAR. In the above situation randomness is involved value in the range randomly that means we have to do till we get a better solution.
In classical HS once the values of controlling parameters are selected they are freezed. The controlling parameters after selecting randomly are freezed for new weight generation. The updating of complex weight continues with with the freezed initial values. In the Improved Harmony Search (IHS) the values of the HMCR and PAR are tuned/updated. In HS for low bound value of PAR with large BW value can leads to degradation performance in finding optimized values and a considerable burden to the iterations in order to find optimum solution[19]. An increment in the PAR and a decrement in HMCR certainly cause harmony variation in the final iteration and lowers the convergence rate and accuracy[24]. HS resembles a random search for PAR value at its higher bound and HMCR value at the lower bound. However, converse selection of PAR and HMCR values tends to decrease the harmony diversity in the last generation, thus, the probability of reaching an optimal solution is reduced. So a modification is a necessary action. This modification is mathematically represented in the following equations(3.1),(3.2).

Input Parameters $W = \begin{pmatrix} w_{1,1} & \cdots & w_{1,HMS} \\ \vdots & \ddots & \vdots \\ w_{N,1} & \cdots & w_{N,HMS} \end{pmatrix}$, HMS, PAR=FCM(0-0.5), HMCR=FCM(0.7-0.99)
Output parameter w_o
Evaluate fitness $F = fitness(W)$, $F = [\ f_1 \quad \ldots \quad f_{HMS}\ ]$
For iter < itermax
|
| if rand() < HMCR
| | W_n = rand(:,HMS)
| else
| | $W_n = W(:, i)$, i=any random integer
| end
| | if rand() < PAR
| | $W_n = W_n + BW$
| | BW = generally range of adjustment
| else
| | $W_n = W_n$+ random pitch
| end
| Evaluate fitness $F_n = fitness(W_n)$, $F = [\ f_1 \quad \ldots \quad f_HMS\ ]$
| $W_o = \begin{cases} W_n & F_n < F \\ W & otherwise \end{cases}$
| $HMCR(it) = 0.99 - (\frac{(0.29+HMCR(it-1))}{1000} * it)$
| $PAR(it) = 0.1 + \frac{(\frac{(0.5-PAR(it-1)}{1000} * it)}{HMS}$
end

Table 3.8: IHS PSEUDO Code

$$HMCR(it) = 0.99 - (\frac{(0.29 + HMCR(it-1))}{1000} * it) \tag{3.1}$$

$$PAR(it) = 0.1 + \frac{(\frac{(0.5-PAR(it-1)}{1000} * it)}{HMS} \tag{3.2}$$

In the above equations(3.1),(3.2) represents the current iteration value. From the above equation it can be concluded that the updated value of the controlling parameters is dependent on the observed value in the previous iteration. Even this improvement suffers an escape from the global optima due to random initialization of the controlling parameters. This problem can be addressed with the support of fuzzy logic rule for initial setting. Fuzzy C-mean Clustering (FCM) is used for the initial selection of the control parameters. FCM will cluster the samples over the given range and gives a single best

PROCESS	HS	IHS
size of populatioin (HMS)	User defined	user defined
Initial population (W)	Random	Random
Considering Rate ($HMCR$) initially	User defined	Value find from Fuzzy C-Mean clustering
Pitch Adjustment (PAR) initially	User defined	Value find from Fuzzy C-Mean clustering
Considering Rate ($HMCR$) after one iteration	Value fixed	Value changes depending on the its previous value
Pitch Adjustment (PAR) after one iteration	Value fixed	Value changes depending on the its previous value

Table 3.9: Comparison and Difference between HS and IHS

cluster value which is used as a initial set value for the HMCR and PAR. The pseudo code and changes/modification in HS heading to a new improved HS that drives to the best solution described clearly in the table3.8 and 3.9.

3.4.1 SIMULATION RESULTS

Considering the linear array geometry the simulation results for multi users and multi interferences are follows by employing Improved Harmony Search (IHS).

Simulation.I

Simulation is conducted for number of users 5 with considering DOA at 10^0 and single interference at 60^0. The simulated adaptive reradiation pattern for the above consideration is as shown in FIg.3.34.

Simulation.II

Simulation is conducted by taking a single interference with 5 users. DOA is considered at 30^0 and interference is at 60^0. The radiation field pattern for this consideration is as shown in Fig.3.35.

Simulation.III

Simulation of the linear array is continued by increasing the number of interference to two and are at $[30^0, 90^0]$. The synthesized radiation pattern of adaptive antenna array is as shown in fig.3.36. For 5 users with considering

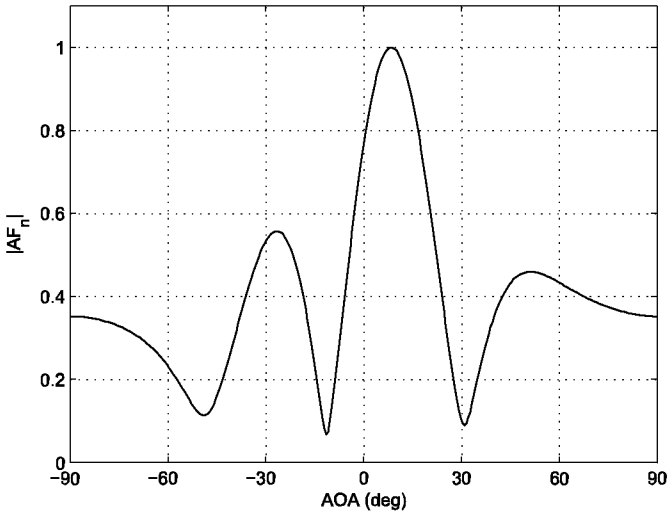

Figure 3.34: Adapted pattern for 5 user with one interference by IHS

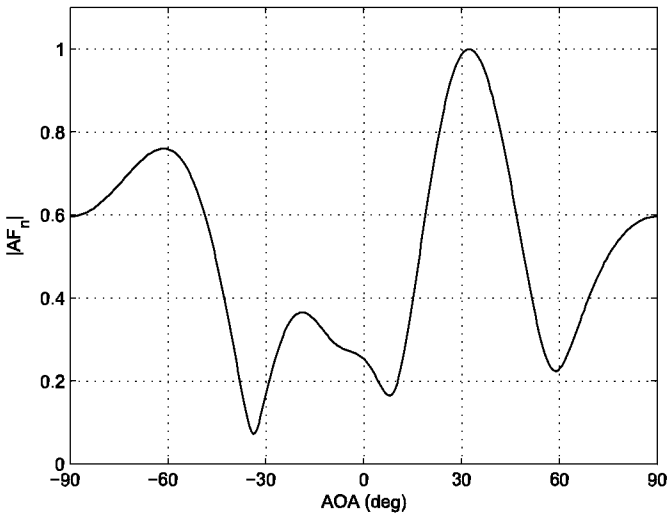

Figure 3.35: Intensity level plot with one interference for 5 users by IHS

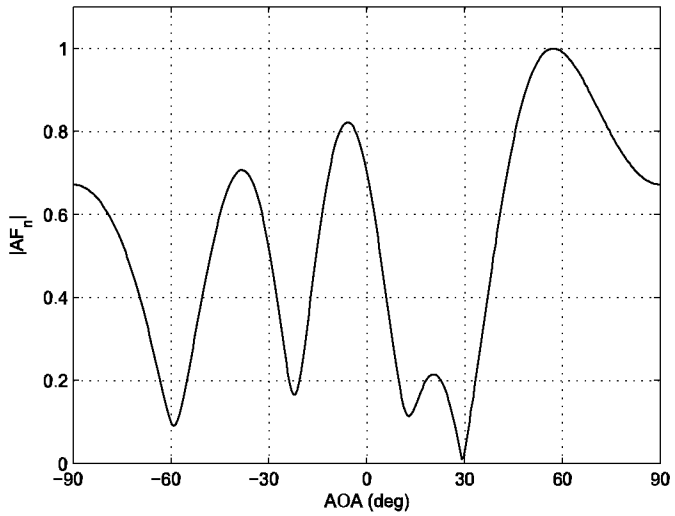

Figure 3.36: Intensity level plot with two interferences for 5 users by IHS

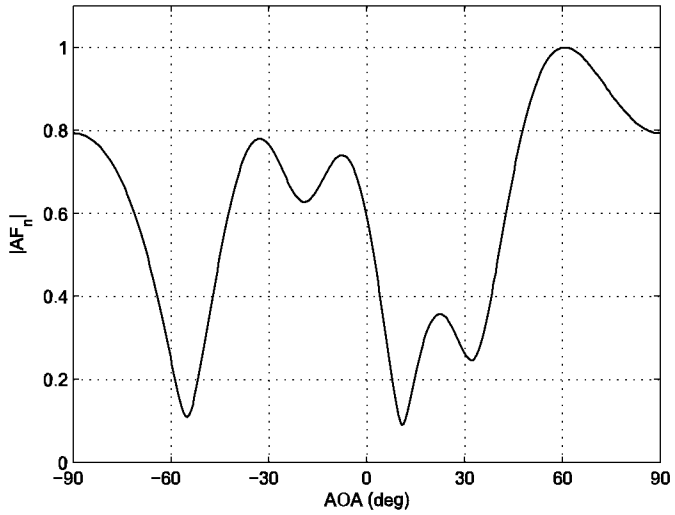

Figure 3.37: Intensity level plot with three interferences for 5 users by IHS

AOA at 60^0.

Simulation.IV

Now the simulation repeated for 5 users with AOA at 60^0, considering three interferences at $[-30^0, -60^0, 30^0]$. The field pattern of the adaptive antenna array with the above considerations is shown in Fig.3.37.

Simulation.V

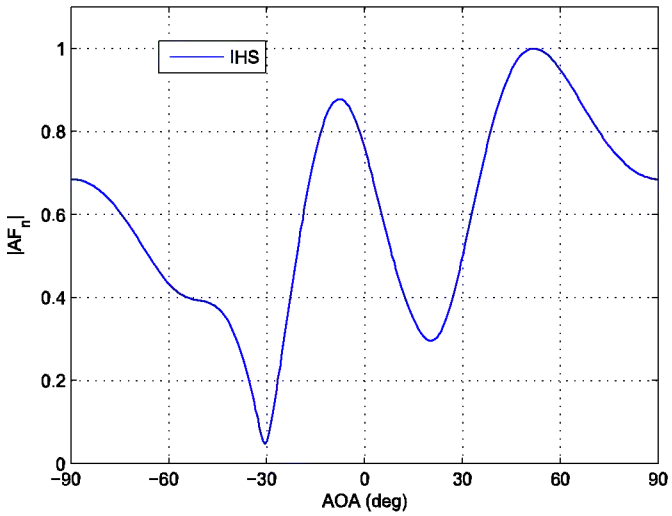

Figure 3.38: Intensity level plot with five interferences for 5 users by HS

For the same number of users the interference level is increased by another two level i.e. in this case interferences considered are 5 and are at $[-30^0, -60^0, 30^0, 90^0, 10^0]$. And AOA is considered at 60^0. The radiation field pattern for the above consideration is as shown in Fig.3.38.

Simulation.VI

Simulation is conducted by taking a single interference initially with 10 users and result is as shown in Fig.3.39. DOA is considered at 10^0 and interference is at 60^0.

Now the simulation is extended to the other geometry which is circular arrangement of the elements. The simulated results for the different cases are shown below.

Simulation I

Simulation is conducted by taking a single interference initially with 5 users and result is as shown in Fig.3.40. DOA is considered at 30^0 and interference is at 60^0.

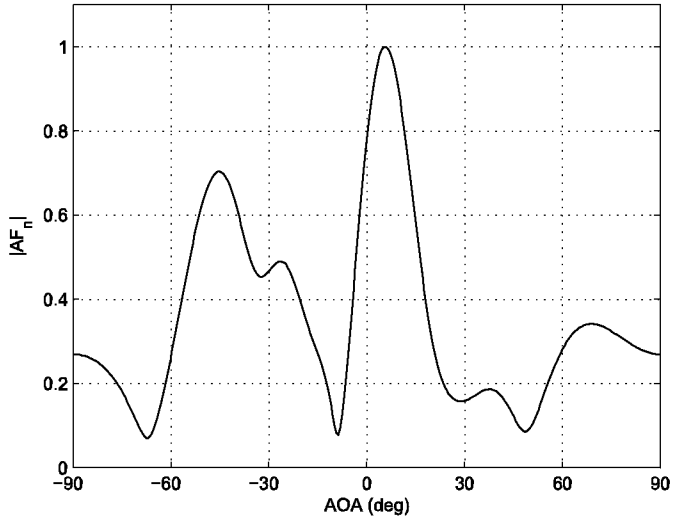

Figure 3.39: Intensity level plot with one interference for 10 users by HS

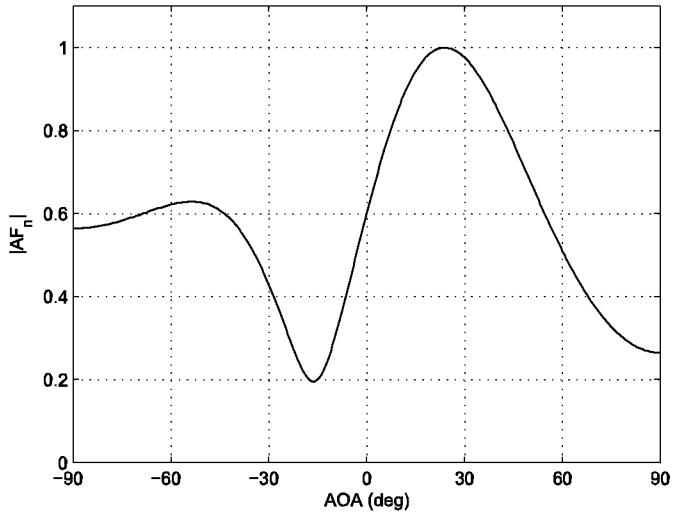

Figure 3.40: Intensity level plot with one interference for 5 users for circular array

Simulation.II

Simulation is conducted by taking a single interference with 5 users and result is as shown in Fig.3.41. DOA is considered at 10^0 and interference is at 60^0.

Simulation.III

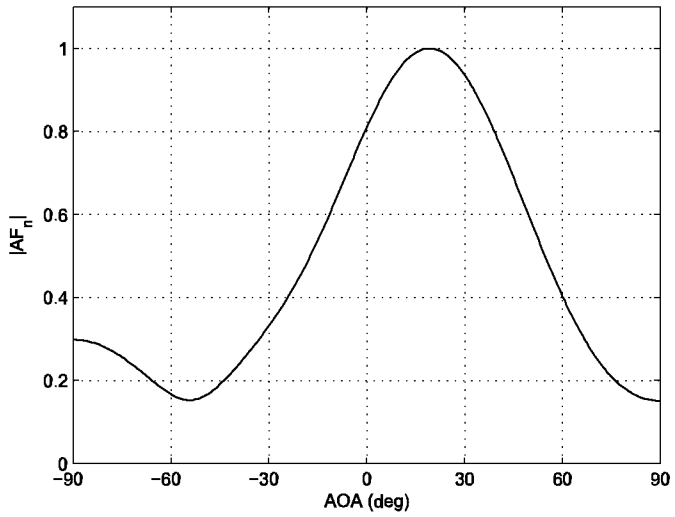

Figure 3.41: Intensity level plot with one interferences for 5 users by IHS

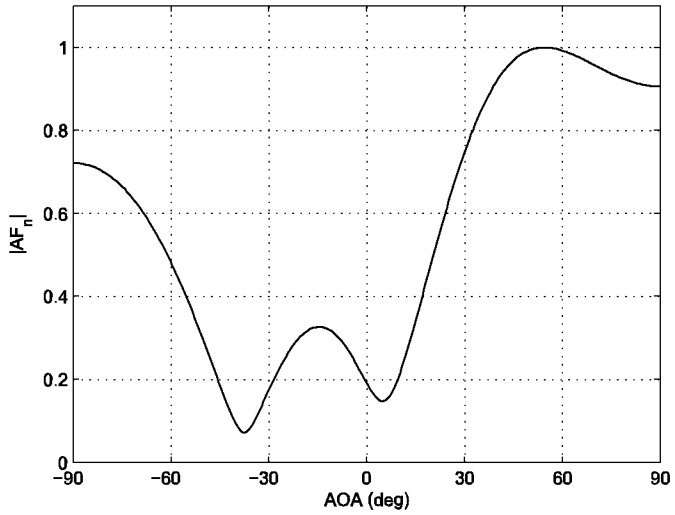

Figure 3.42: Intensity level plot with five interferences for 5 users

For the same number of users the interference level is increased by another one level i.e. in this case interferences considered are 5 and are at $[-30^0, -60^0, 30^0, 90^0, 10^0]$. And AOA is considered at 60^0. The radiation field pattern for the above consideration is as shown in Fig.3.42.

Simulation.IV

Simulation is conducted by taking a single interference initially with 10 users

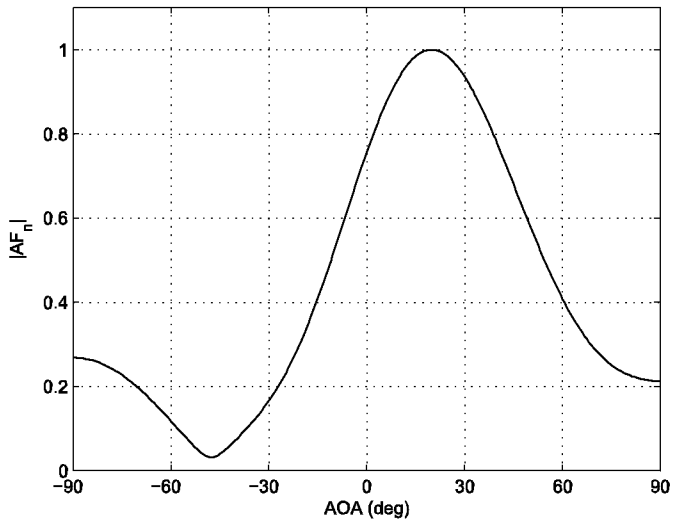

Figure 3.43: Intensity level plot with one interference for 10 users by IHS

and result is as shown in Fig.3.43. DOA is considered at 10^0 and interference is at 60^0.

3.5 COMPARISON OF HS AND IHS

LINEAR ARRANGEMENT

Simulation.I

Simulation is conducted for number of users 5 with considering DOA at 10^0 and single interference at 60^0. The simulated adaptive reradiation pattern for the above consideration is as shown in FIg.3.44.

The Fig.3.44 gives the field pattern for the above considerations and clears that the beam width by using IHS is increased and the interference level is decreased comparatively than HS.

Simulation.II

Simulation is conducted by taking a single interference with 5 users. DOA is considered at 30^0 and interference is at 60^0. The radiation field pattern for

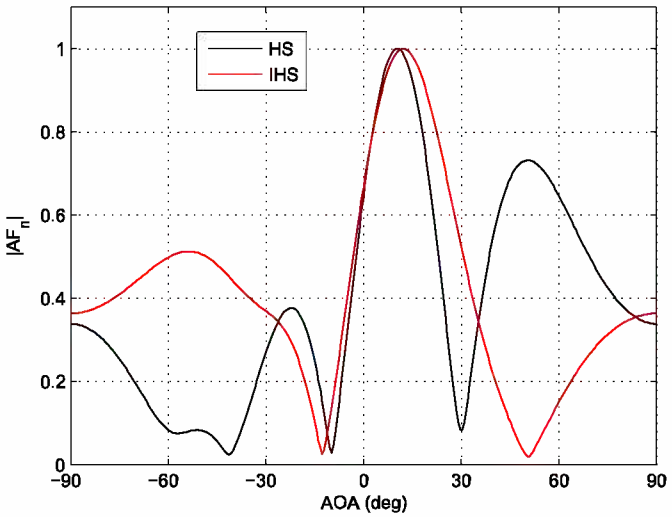

Figure 3.44: Adapted pattern for 5 user with one interference

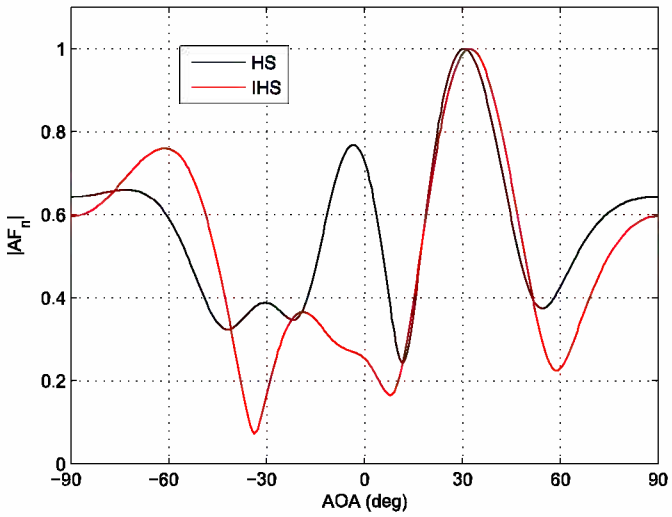

Figure 3.45: Intensity level plot with one interference for 5 users

this consideration is as shown in Fig.3.45.

From Fig.3.45 the adaptiveness of the IHS is performs well than the HS. The interference level has been decreased comparative with HS.

Simulation.III

Simulation of the linear array is continued by increasing the number of interference to two and are at $[30^0, 90^0]$. The synthesized radiation pattern of

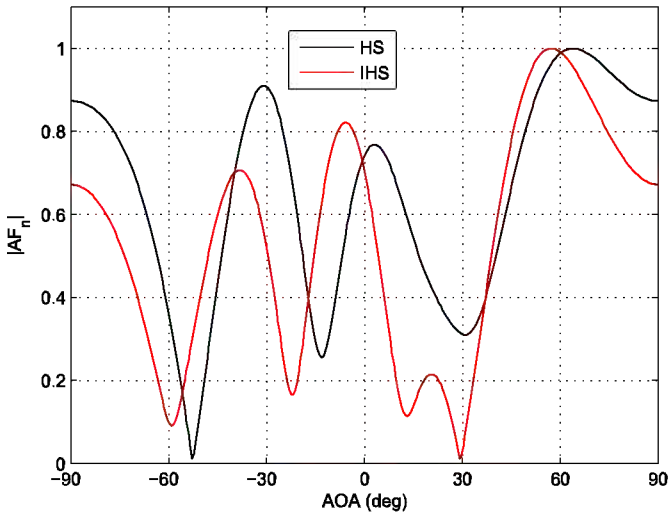

Figure 3.46: Intensity level plot with two interferences for 5 users

adaptive antenna array is as shown in fig.3.46. For 5 users with considering AOA at 60^0.

From the graphical representation of field pattern in the Fig.3.46 represents for the interferences IHS is working good and the AOA detection is in satisfied level.

Simulation.IV

Now the simulation repeated for 5 users with AOA at 60^0, considering three interferences at $[-30^0, -60^0, 30^0]$. The field pattern of the adaptive antenna array with the above considerations is shown in Fig.3.47.

In this case the radiation pattern in the Fig.3.47 clears that the both techniques performs well for this consideration.

Simulation.V

For the same number of users the interference level is increased by another two level i.e. in this case interferences considered are 5 and are at $[-30^0, -60^0, 30^0, 90^0, 10^0]$. And AOA is considered at 60^0. The radiation field pattern for the above consideration is as shown in Fig.3.48.

In this case we have increased the number of interference for this case AOA

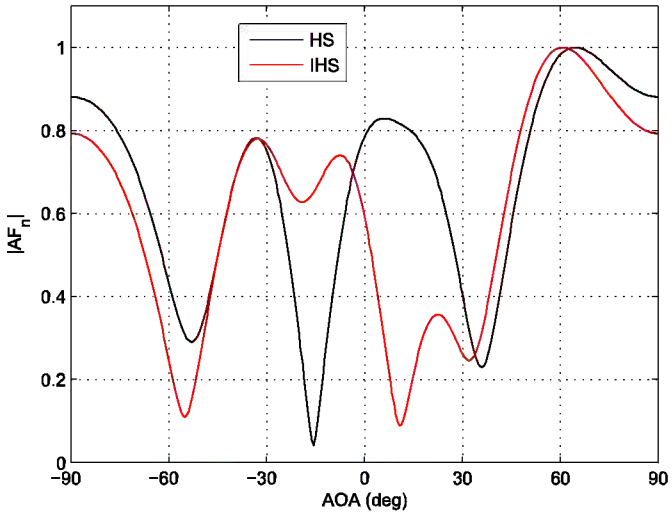

Figure 3.47: Intensity level plot with three interferences for 5 users

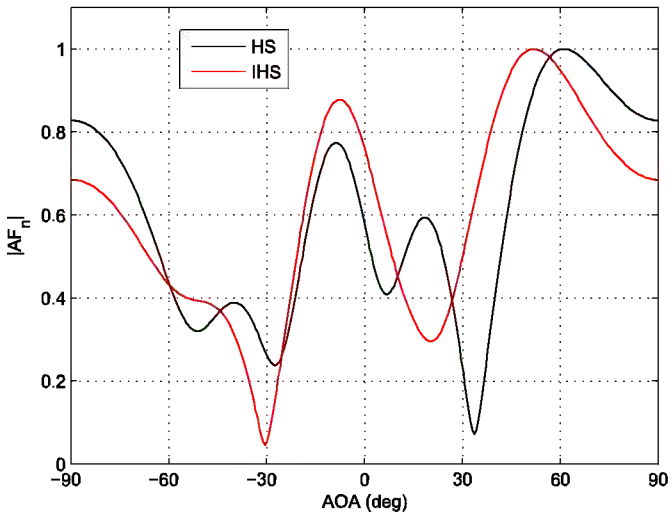

Figure 3.48: Intensity level plot with five interferences for 5 users

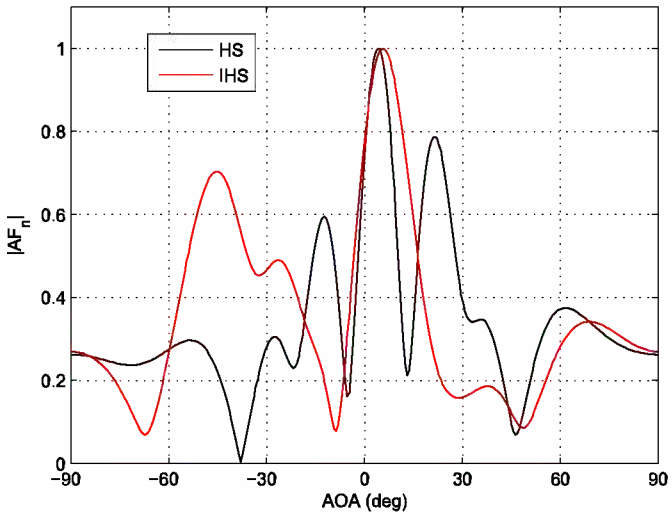

Figure 3.49: Intensity level plot with one interference for 10 users

detection is satisfied in HS and interference levels are satisfied in IHS.

Simulation.VI

Simulation is conducted by taking a single interference initially with 10 users and result is as shown in Fig.3.49. DOA is considered at 10^0 and interference is at 60^0.

As the user number increases the working of IHS is as same in before cases. i.e. the interference level is decreased compared to HS.

CIRCULAR ARRANGEMENT

Simulation I

Simulation is conducted by taking a single interference initially with 5 users and result is as shown in Fig.3.50. DOA is considered at 30^0 and interference is at 60^0.

From the Fig.3.50 we can convey that the IHS is working well for objective and that objective is interference objective also DOA is in satisfied level.

USER	AOA(in^0)	AOI(in^0)	OPTIMIZED COMPLEX EXCITATIONS (HS)	OPTIMIZED COMPLEX EXCITATION (IHS)
5	10	60	[-0.6838-0.4596i -0.0633-0.8502i 0.0349-0.0323i 0.4337-0.8506i 1+0i]	[0.1616-0.1332i 0.3039-0.1961i 1+0i 0.1324+0.3385i 0.0370+0.9827i]
5	30	60	[0.0210+0.9747i -0.6479+0.1684i 1+0i 0.5389+0.0517i 0.0714+0.8607i]	0.3761-0.5628i 0.0159+0.8663i -0.0838+0.6434i -0.6796-0.3756i 1+0i]
5	60	30, 90,	-0.3464+0.6024i 1+0i 0.3214+0.5934i -0.3719-0.1546i -0.0494+0.7904i]	1+0i -0.0865-0.2712i 0.3224-0.5427i 0.2665+0.3770i 0.0595-0.8248i]
5	60	-30,-60,30	[1+0i 0.1747+0.4309i 0.0364+0.0188i 0.0063+0.9043i 0.2688-0.3530i]	[0.1384+0.5469i -0.1856-0.3263i 0.0986+0.7745i 0.1946+0.3085i 1+0i]
5	60	-30 60,30,90,10	[-0.2057+0.7795i -0.0556-0.6237i 0.4330+0.6120i 0.4750-0.2956i 1+0i]	[0.224+0.4622i 0.0229-0.7657i 1+0i 0.07861-0.2347i 0.1440-0.4750i]
10	10	60	[-0.0171-0.3237i 0.0856-0.8662i 0.0029-0.4531i 0.2309-0.2012i 0.5153+0.2222i 0.0709+0.4881i 0.3072-0.2445i 0.2523-0.0879i 1+0i 0.2218+0.2871i]	[-0.1482-0.1693i -0.0927+0.1226i -0.1048-0.5071i -0.2253-0.2326i 0.1841-0.5772i -0.04-0.6273i 0.1362-0.0404i 1+0i 0.1280-0.2796i -0.0429-0.0647i]

Table 3.10: Optimized complex weights for the linear geometry for different scenarios

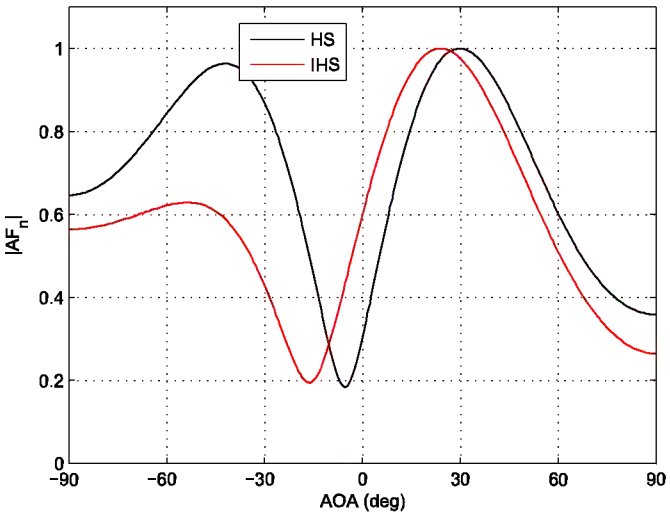

Figure 3.50: Intensity level plot with one interference for 5 users for circular array

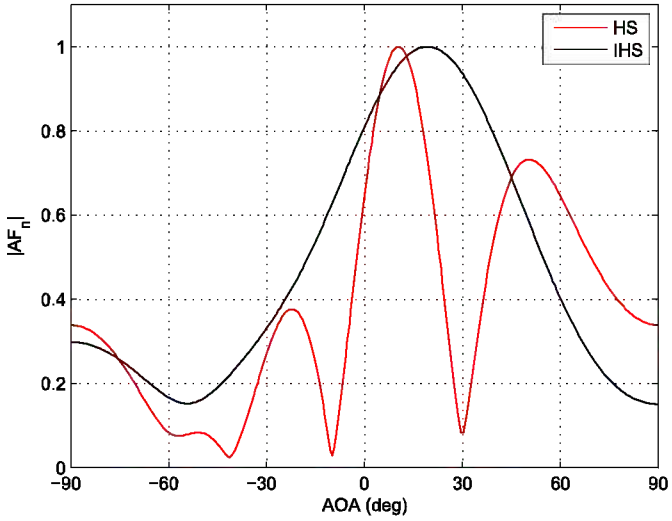

Figure 3.51: Intensity level plot with one interferences for 5 users by IHS

Simulation.II

Simulation is conducted by taking a single interference with 5 users and result is as shown in Fig.3.51. DOA is considered at 10^0 and interference is at 60^0.

From the Fig.3.51 IHS is satisfying one objective perfectly even HS also satisfies one objective.

Simulation.III

For the same number of users the interference level is increased by another one level i.e. in this case interferences considered are 5 and are at $[-30^0, -60^0, 30^0, 90^0, 10^0]$. And AOA is considered at 60^0. The radiation field pattern for the above consideration is as shown in Fig.3.52.

From the graphical representation of radiation field in Fig.3.52 shows that the interference levels in this case are minimized using IHS and by using the beam width at the DOA is high comparting with HS.

Simulation.IV

Simulation is conducted by taking a single interference initially with 10 users

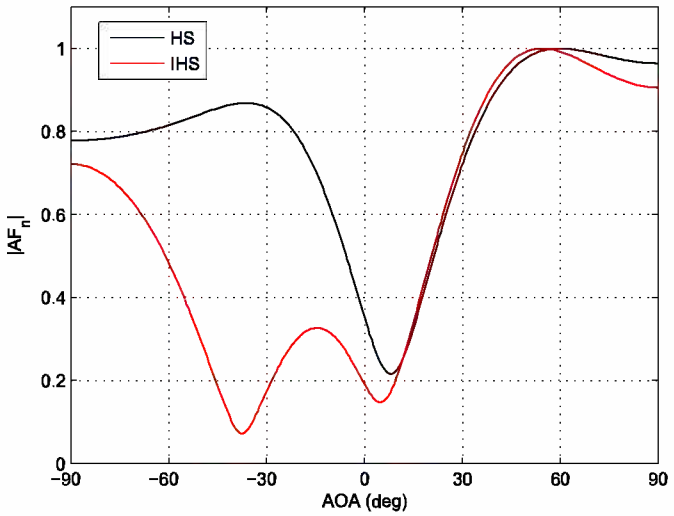

Figure 3.52: Intensity level plot with five interferences for 5 users

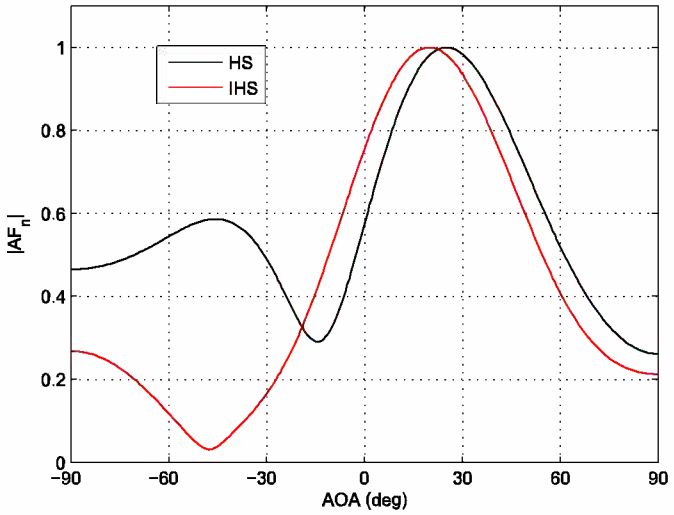

Figure 3.53: Intensity level plot with one interference for 10 users by IHS

and result is as shown in Fig.3.53. DOA is considered at 10^0 and interference is at 60^0.

From the Fig.3.53 the IHS is outforms well than the HS.
IHS is works better for the minimization of the interference levels with high beam width at DOA.
Both the adaptive techniques performance measurement in achieving 0db at

USER	AOA(in^0)	AOI(in^0)	OPTIMIZED COMPLEX EXCITATIONS (HS)	OPTIMIZED COMPLEX EXCITATION (IHS)
5	10	60	[-0.4918+0.4255i -0.3645-0.5357i 0.1726-0.2198i 1+0i -0.0278-0.9742i]	[0.1616-0.1332i 0.3039-0.1961i 1+0i 0.1324+0.3385i 0.0370+0.9827i]
5	30	60	[1+0i 0.1893+0.0687i 0.06750+0.7296i 0.1855+0.4553i 0.2333+0.6221i]	[0.3761-0.5628i 0.0159+0.8663i -0.0838+0.6434i -0.6796-0.3756i 1+0i]
5	60	-30 60,30,90,10	[0.1198- 0.2270i 1+0i 0.2552-0.4956i 0.0462-0.9075i -0.3656-0.3033i]	[0.224+0.4622i 0.0229-0.7657i 1+0i 0.07861-0.2347i 0.1440-0.4750i]
10	10	60	[-0.2123-0.9212i 0.1462-0.6589i 0.0736+0.3687i 0.0339+0.0324i 0.0873-0.0951i 0.4333+0.2128i 0.3366-0.1447i 1+0i 0.3490-0.3007i 0.3375-0.1717i]	[-0.1482-0.1693i 0.0927+0.1226i -0.1048-0.5071i -0.2253-0.2326i 0.1841-0.5772i -0.04-0.6273i 0.1362-0.0404i 1+0i 0.1280-0.2796i -0.0429-0.0647i]

Table 3.11: Optimized complex weights for the circular geometry for different scenarios

	users	AOA(in^0)	AOI(in^0)	HS ($indB$)	IHS ($indB$)
LINEAR	5	10	60	0.6	0.2
	5	30	60	0.4	0.2
	5	60	30,90	0.3, 0.9	0, 0.7
	5	60	-30, -60, 30	0.78, 0.4, 0.4	0.78, 0.3, 0.8
	5	60	-30, -60, 30, 90,	0.25, 0.4, 0.2, 0.85, 0.75	0.1, 0.4, 0.4, 0.7, 0.42
	10	10	60	0.4	0.6
CIRCULAR	5	10	60	0.4	0.5
	5	30	60	0.6	0.5
	5	60	-30, -60, 30, 90, 10	0.9, 0.8, 0.7, 0.9, 0.2	0.2, 0.5, 0.7, 0.9, 0.15
	10	10	60	0.5	0.4

Table 3.12: Representation of intensity level at the interferences

the angle of inference failed. On a comparative analysis the radiation spilled over at the inference angle/angles for multi users has been analyzed. The statistical table comprises the percentage of radiated power at the interference angles tabled in table3.13. Lower the power better is the performance.

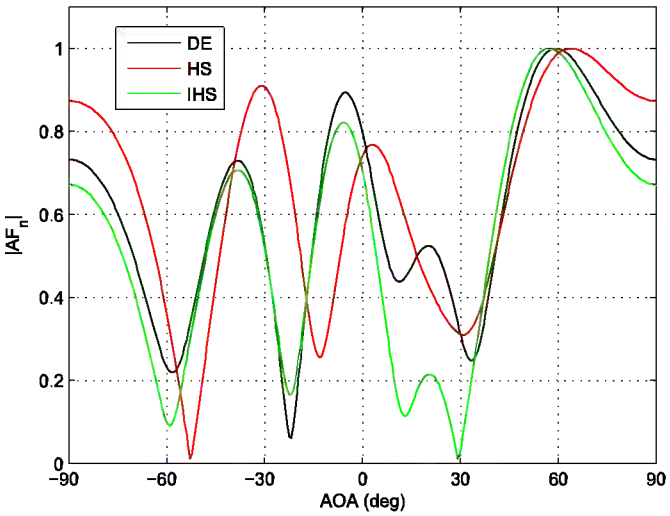

Figure 3.54: Comparison with 1 interference with 5 users

3.6 COMPARISON OF DE, HS and IHS

In this section the discussion is about the comparison between the evolutionary techniques DE HS and IHS. This comparison is made for the both geometrical arrangement those are linear element arrangement and circular element arrangement. In the below discussion initial four simulations are for linear arrangement of the elements, and the remaining 2 simulation are for the circular arrangement of the elements.

Simulation.I

Simulation of the linear array is continued by increasing the number of interference to two and are at $[30^0, 90^0]$. The synthesized radiation pattern of adaptive antenna array is as shown in fig.3.54. For 5 users with considering AOA at 60^0.

The graphical analysis clears that IHS outperforms DE and HS in the accurate detection of the main beam. In IHS intensity level at interferences is lower than DE and HS.

Simulation.II

Now the simulation repeated for 5 users with AOA at 60^0, considering three interferences at $[-30^0, -60^0, 30^0]$. The field pattern of the adaptive antenna

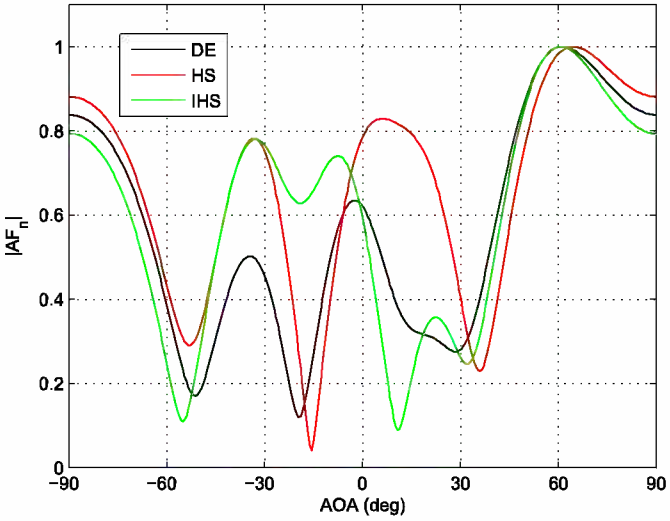

Figure 3.55: Comparison with 3 interference with 5 users

array with the above considerations is shown in Fig.3.55.

Fig.3.29 gives the stability of DE and IHS in detecting the AOA and AOI which are the main objectives.However in HS technique accuracy in detection is not maintained.

Simulation.III

For the same number of users the interference level is increased by another two level i.e. in this case interferences considered are 5 and are at $[-30^0, -60^0, 30^0, 90^0, 10^0]$. And AOA is considered at 60^0. The radiation field pattern for the above consideration is as shown in Fig.3.56.

Fig3.56 shows the fact that with a rapid increase in the interferences IHS, HS and DE is not consistent in accurately detecting all the interferences. But the AOA detection objective is satisfied by both the techniques HS and DE but not in IHS.

Simulation.IV

Performance comparison of both the algorithms for 10^0 numbers of users and considering one-interference at 60^0 and AOA at 10^0 is done. As the increment in number of users from the fig.3.58 one can observe that AOA location is better in DE but not at AOI.

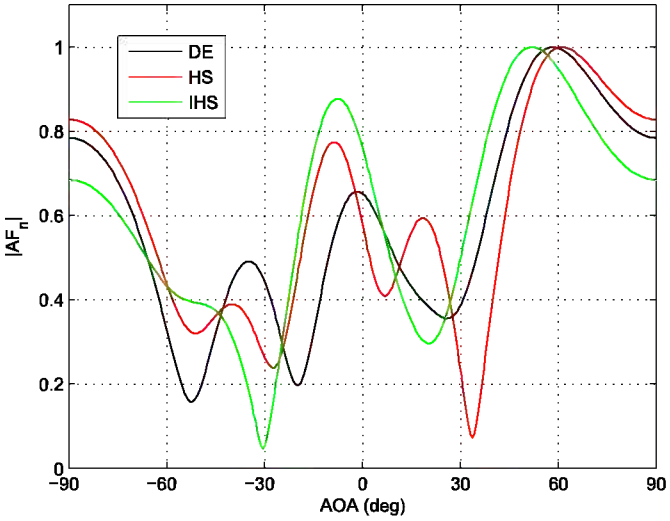

Figure 3.56: Comparison with 5 interference with 5 users

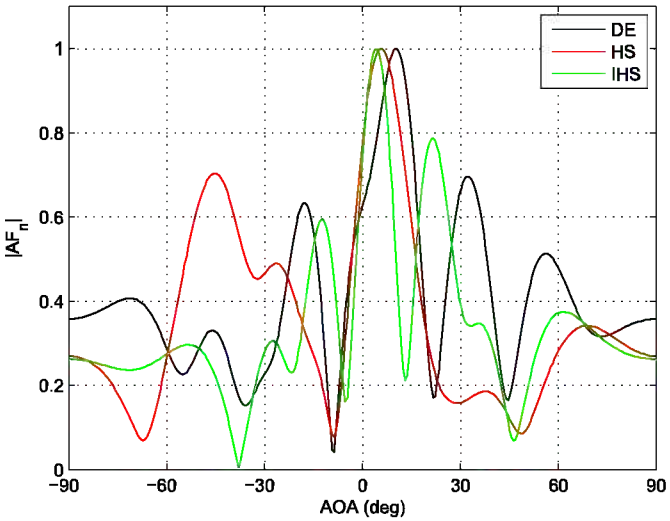

Figure 3.57: Comparison with 1 interference with 10 users

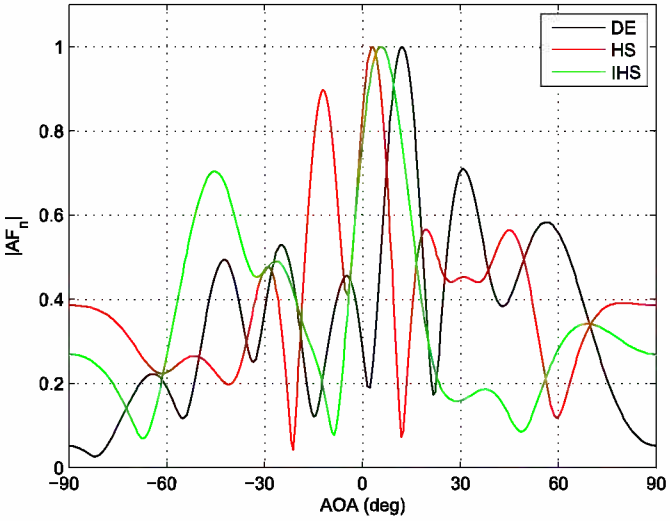

Figure 3.58: Comparison with 1 interference with 10 users

Simulation.V

Simulation is continued for circular array by increasing the number of users to 10 and decreasing the number of interferences from 10 to 1. AOA is 10^0 and AOI is 60^0.

The graphical analysis of the field pattern in the Fig.3.58 concludes a circular arrangement though optimized with powerful evolutionary tools does not meet the multiple objectives. It gives an insight of wider beam coverage.

Simulation.VI

Continuation of the simulation further to the circular array and comparing the both algorithms is taken up. Five number of users with AOA at 60^0 and the number of interferences are 5 and are at $[-30^0, -60^0, 30^0, 90^0, 10^0]$. The radiation pattern of both techniques are shown in Fig3.59.

From the above different scenarios it is observed that DE performance for detecting AOA is considerable good compared to other two techniques. However, the use of IHS leads to a low level intensity at interferences (AOI).

On a comparative analysis the radiation spilled over at the inference angle/angles for multi users has been analyzed. The statistical table comprises the percentage of radiated power at the interference angles shown in table3.13.

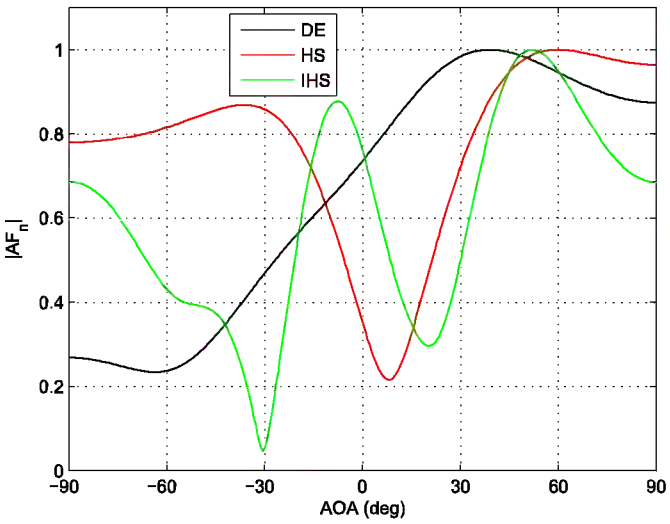

Figure 3.59: Comparison with 5 interference with 5 users

	users	AOA(in^0)	AOI(in^0)	DE ($indB$)	HS ($indB$)	IHS ($indB$)
LINEAR	5	60	30,90	0.3, 0.7	0.3, 0.9	0, 0.7
	5	60	-30, -60, 30	0.45, 0.4, 0.3	0.78, 0.4, 0.4	0.7, 0.2, 0.22
	5	60	-30, -60, 30, 90, 10	0.42, 0.3, 0.4 0.8, 0.55	0.25, 0.4, 0.2, 0.85, 0.75	0, 0.4, 0.4, 0.7, 0.4
	10	10	60	0.5	0.2	0.35
CIRCULAR	5	60	-30, -60, 30, 90, 10	0.5, 0.25, 0.9, 0.85, 0.8	0.9, 0.8, 0.7, 0.9, 0.2	0.2, 0.4, 0.4, 0.7, 0.4
	10	10	60	0.45	0.6	0.3

Table 3.13: Representation of intensity level for DE HS and IHS at the interferences

Chapter 4

CONCLUSION AND FUTURE SCOPE

Smart antennas are the antennas in which the main beam is steered to the angle of direction and suppress the intensity level at the interference angles. In this work smart antenna system is designed and adapted using intelligent techniques for multi-users multi-interferences. The evolutionary techniques used are DE, HS and IHS. The following conclusions can be drawn based on the simulation results of these techniques.

4.1 Conclusion

- In this thesis adaptive beam forming for linear and circular geometry using different evolutionary tools (Differential Evolution, Harmony Search and Modified Harmony search) for a multiple objective function is considered. The evolutionary techniques are remodeled, establishing the analogy between the bio-inspired parameters and the antenna parameters.
- Different case studies including single and multi-interference for multi-user concludes that DE technique stretches out in a better manner for the considered objectives.
- The performance of HS is concentrates or ranked better for a single objective.

- Another conclusion can be drawn based on the computational time and algorithm parametric complexity which portrait DE as a better technique over HS.
- An attempt is made to improvise the technicality of HS and boost up its performance.
- Usage of IHS leads a low intensity level at the interferences compared to DE and HS.
- A linear and circular antenna array is modeled using CST (Computer Simulation Technology) and based on this design a prototype are fabricated.

4.2 Limitations and Future Scope

- Through out the work the mutual coupling between the antenna array elements is neglected.
- Smart antenna array geometries are limited to only linear and circular shape.
- A neuro-fuzzy approach can be experimented to set initial parameters.
- Similar antenna elements has been considered non-identical.
- DE algorithm standard ones. A lot of scope for the development of algorithm.
- The objective is limited to DOA and AOI. New objectives can be incorporated and extended.

Bibliography

[1] JR Joseph C. Liberti and Theodore S. Rappaport. Smart antennas for wireless communications. *Prentice Hall communications engineering and emerging technologies series*, 1999.

[2] Constantine A Balanis. *Antenna theory: analysis and design.* Wiley-Interscience, 2012.

[3] Ahmed El Zooghby. Smart antenna engineering, 2005 artech house. *INC., Norwood.*

[4] Magdalena salazar-Palma Tapan K.Sarkar, Michel C.Wicks and Robert J.Bonneau. *Smart Antennas.* Wiley-Interscience, 2003.

[5] Huilong Zhang, Xiurong Ma, Yunxiang Cheng, and Yuan Bai. Study on doa estimation algorithm for smart antenna of uniform circular. In *Computer Application and System Modeling (ICCASM), 2010 International Conference on*, volume 15, pages V15–627. IEEE, 2010.

[6] Lal Chand Godara. *Smart antennas*, volume 15. CRC press, 2004.

[7] Zaharias D Zaharis, Christos Skeberis, and Thomas D Xenos. Improved antenna array adaptive beamforming with low side lobe level using a novel adaptive invasive weed optimization method. *Progress In Electromagnetics Research*, 124:137–150, 2012.

[8] Wenyi Wang, Renbiao Wu, and Junli Liang. A novel diagonal loading method for robust adaptive beamforming. *Progress In Electromagnetics Research C*, 18:245–255, 2011.

[9] AK Qin, VL Huang, and PN Suganthan. Differential evolution algorithm with strategy adaptation for global numerical optimization. *Evolutionary Computation, IEEE Transactions on*, 13(2):398–417, 2009.

[10] Rammohan Mallipeddi, Joni Polili Lie, PN Suganthan, Sirajudeen Gulam Razul, and Chong Meng S See. Near optimal robust adaptive beamforming approach based on evolutionary algorithm. *Progress In Electromagnetics Research B*, 29:157–174, 2011.

[11] Rainer Storn. On the usage of differential evolution for function optimization. *NAFIPS*, pages 519–523, 1996.

[12] Rainer Storn and Kenneth Price. Differential evolution - a simple and efficient adaptive scheme for global optimization over continuous spaces. *Technical Report TR-95-012*, March 1995.

[13] Rainer Storn and Kenneth Price. Differential evolution a simple evolution strategy for fast optimization. *Dr. Dobb's*, (03):1824 and 78, April 1997.

[14] R Mallipeddi, PN Suganthan, QK Pan, and MF Tasgetiren. Differential evolution algorithm with ensemble of parameters and mutation strategies. *Applied Soft Computing*, 11(2):1679–1696, 2011.

[15] Zong Woo Geem, Joong Hoon Kim, and GV Loganathan. A new heuristic optimization algorithm: harmony search. *Simulation*, 76(2):60–68, 2001.

[16] Kang Seok Lee and Zong Woo Geem. A new meta-heuristic algorithm for continuous engineering optimization: harmony search theory and practice. *Computer methods in applied mechanics and engineering*, 194(36):3902–3933, 2005.

[17] Ren Diao and Qiang Shen. Two new approaches to feature selection with harmony search. In *Fuzzy Systems (FUZZ), 2010 IEEE International Conference on*, pages 1–7. IEEE, 2010.

[18] Swagatam Das, Arpan Mukhopadhyay, Anwit Roy, Ajith Abraham, and Bijaya K Panigrahi. Exploratory power of the harmony search algorithm: analysis and improvements for global numerical optimization. *Systems, Man, and Cybernetics, Part B: Cybernetics, IEEE Transactions on*, 41(1):89–106, 2011.

[19] M Mahdavi, M Fesanghary, and E Damangir. An improved harmony search algorithm for solving optimization problems. *Applied mathematics and computation*, 188(2):1567–1579, 2007.

[20] Mahamed GH Omran and Mehrdad Mahdavi. Global-best harmony search. *Applied Mathematics and Computation*, 198(2):643–656, 2008.

[21] Lucas M Pavelski, Carolina P Almeida, and Richard A Gonçalves. Harmony search for multi-objective optimization. In *Neural Networks (SBRN), 2012 Brazilian Symposium on*, pages 220–225. IEEE, 2012.

[22] Robert S.Elliott. *ANTENNA THEORY AND DESIGN*. John Wiley and Sons, Ltd, 2005.

[23] Ling Wang, Yin Xu, Yunfei Mao, and Minrui Fei. A discrete harmony search algorithm. In *Life System Modeling and Intelligent Computing*, pages 37–43. Springer, 2010.

[24] Hadi Sarvari and Kamran Zamanifar. A self-adaptive harmony search algorithm for engineering and reliability problems. In *Computational Intelligence, Modelling and Simulation (CIMSiM), 2010 Second International Conference on*, pages 59–64. IEEE, 2010.

[25] Ponnuthurai N Suganthan, Nikolaus Hansen, Jing J Liang, Kalyanmoy Deb, YP Chen, Anne Auger, and S Tiwari. Problem definitions and evaluation criteria for the cec 2005 special session on real-parameter optimization. *KanGAL Report*, 2005005, 2005.

[26] Constantinos Votis, Vasilis Christofilakis, and Panos Kostarakis. Geometry aspects and experimental results of a printed dipole antenna. *International Journal Communications, Net-work and System Sciences*, 3(2):97–100, 2010.

Appendix A

Appendix-I

In this section, we provide the results of testing the performance of HS and DE over six representative benchmark functions from the test suite of the Congress on Evolutionary Computation (CEC) 2005 Special Session and Competition on Real Parameter Optimization[25]. All the benchmarks have been tested for dimensions D=30, independent runs of each of the algorithms were carried out and the average and the computing time for each algorithm and the number of iterations to obtain the least fitness is noted down. Absolute runtime and number of iterations of standard functions are tabulated. TableA.1 is a statistical comparison on the performance of the two algorithms in terms of computing time and number of iterations required to reach a least fitness (zero). To have a fair comparison both the initial population size are set for the same value. The table gives us that the computational time required for DE HS and MHS for minimizing the four testing equations. From the tableA.1 it shows that the optimization techniques are converged and can be used for the minimizing the objective function.

Test Function	equation		DE	HS	MHS
ROSENBROCK'S equation	$f(x,y) = (1-x)^2 +100(y-x^2)^2$	N	2	2	2
		FITNESS	0	0	0
		ITERATIONS	1592	8636	6451
		CPU TIME(sec)	0.1872	574.504	465.1170
GRIEWANK'S equation	$f(x) = 1 + \frac{1}{400}\sum_{i=1}^{n} x_i^2 - \prod_{i=1}^{n} \cos\frac{x_i}{\sqrt{i}}$	N	30	30	30
		FITNESS	0	0	0
		ITERATIONS	2501	2710	2664
		CPU TIME(sec)	0.1825	176.6243	166.0471
ACKLEY'S equation	$f(x) = -20\exp^{-\frac{1}{5}\sqrt{\frac{1}{n}\sum_{i=1}^{n} x_i^2}} - \exp^{-\frac{1}{n}\sum_{i=1}^{n}\cos 2\pi x_i} +20 + e$	N	30	30	30
		FITNESS	0	0	0
		ITERATIONS	5960	6153	6451
		CPU TIME(sec)	4.3368	103.3195	96.1170
RASTIGIN'S equation	$f(x) = \sum_{i=1}^{n}(x_i^2 - A\cos 2\pi x_i) +An$	N	30	30	30
		FITNESS	0	0	0
		ITERATIONS	9548	8198	9751
		CPU TIME(sec)	6.9108	551.2919	461.5791

Table A.1: Run Time and fitness comparison of standard functions

Appendix B

Appendix-II

Computer Simulation Technology (CST) is a full-featured software package for electromagnetic analysis and design in the high frequency range. CST provides different solvers for different applications. It has four simulation techniques they are Transient solver(TS), Frequency domain solver(DMS), Integral equation solver(IES) and Eigenmode solver(ES). In these the most flexible and mostly used for antenna analysis solver is TS. Prototypes of this thesis are developed using this software.

In CST by using TS the far field pattern is observed for the linear and circular arrangement of the 5 elements. The dimensions of the patch dipole are calculated for the fixed frequency(f). For calculation of dimensions we need to consider a metal for substrate whose dielectric constant(ϵ_r) value is known and thickness(h) has to be decided. Since as the value of dielectric constant value increases the loss is more so consider the metal with low dielectric constant value. The calculation of the length and width of the dipole patch are as follow[26]

$$\lambda_0 = \frac{c}{f}$$

Guide wave length

$$\lambda_d = \frac{\lambda_0}{\sqrt{\epsilon_r}}$$

$$p = \log\left(\frac{\lambda_d}{0.1016 * \lambda_0}\right) - 1$$

Width of antenna

$$W = h * \lambda_d * p$$

Strip width

$$w_s = \sqrt{W}$$

$$U = \frac{w_s}{h}$$

Effective dielectric constant

$$\epsilon_{ef} = \frac{\epsilon_r + 1}{2} + \frac{\epsilon_r - 1}{2}[1 + \frac{10}{U}]^a b$$

where

$$a = 1 + \frac{1}{49}\ln\left[\frac{U^4 + (U/52)^2}{U^4 + 0.432}\right] + \frac{1}{18.7}\ln\frac{U}{81}^3$$

$$b = 0.564[\frac{\epsilon_r - 0.9}{\epsilon_r + 0.3}]^{0.053}$$

Effective change in length due to effective dielectric constant

$$\Delta L = 0.412 * h\frac{\epsilon_r + 0.3}{\epsilon_r - 0.258}\frac{w_s/h + 0.264}{w_s/h + 0.813}$$

Length of dipole is

$$L = \left(\frac{c}{2f * \sqrt{\epsilon_{ef}}}\right) - 2\Delta L$$

Width of dipole is

$$W = L/3$$

From the above equations one can able to find the length and width of the dipole patch by fixing the frequency and dielectric constant. By considering the frequency $2.4GHz$ and the metal considered is Teflon whose dielectric constant value is 2.1 with thickness of $2mm$. The prototypes made with above considerations are shown in below figures. The dipole patch linear arrangements are shown in Fig.B.1 and Fig.B.2. The circular arrangement of the 5 dipole elements are shown in Fig.B.3 and Fig.B.4. Those figures shows the front and back views of the design.

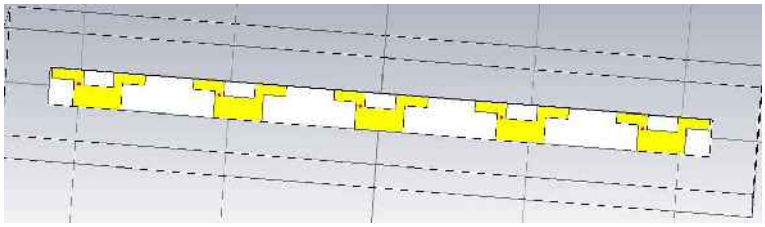

Figure B.1: Printed Linear Dipole Patch Front view

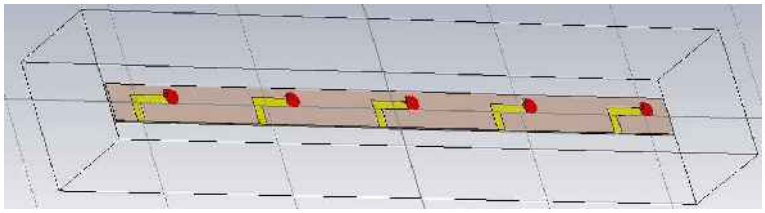

Figure B.2: Printed Linear Dipole Patch Front view

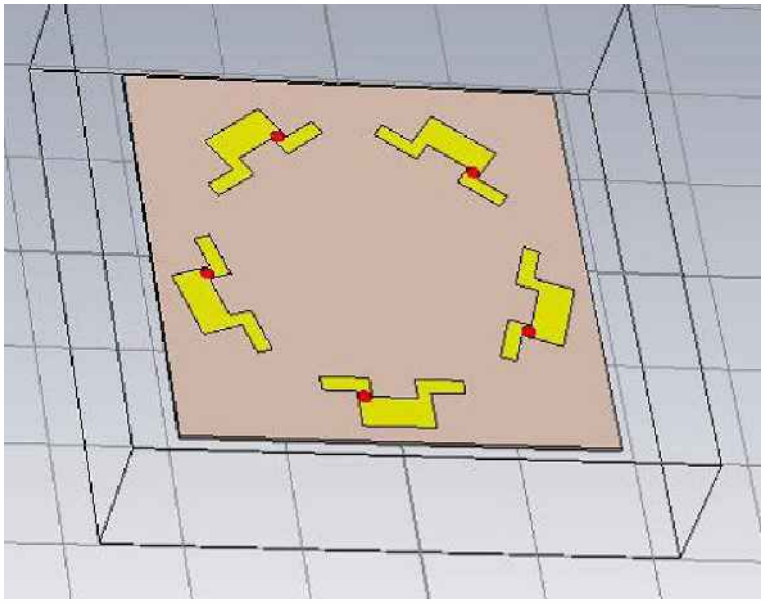

Figure B.3: Printed Circular Dipole Patch Front view

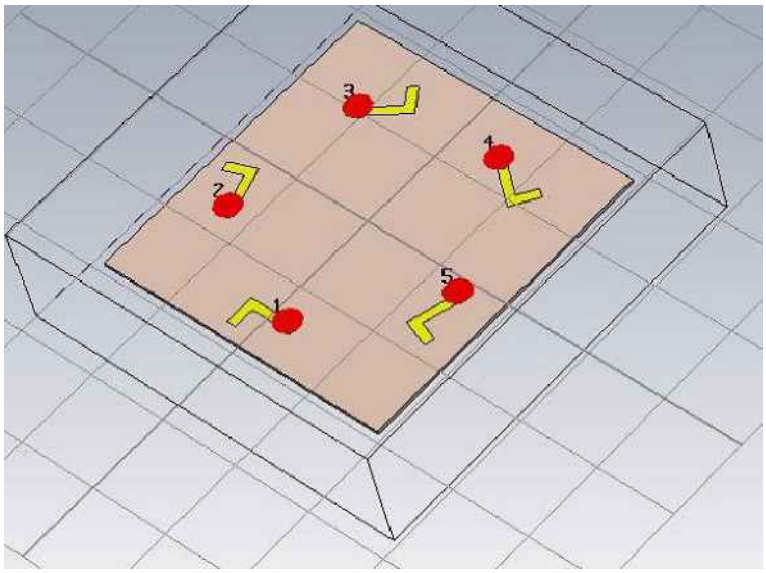

Figure B.4: Printed Circular Dipole Patch Front view

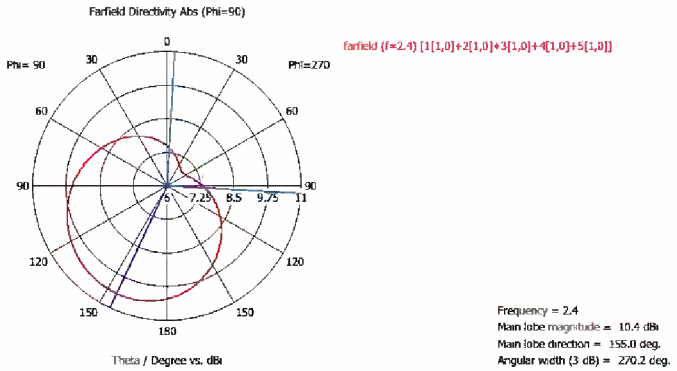

Figure B.5: Printed Linear Dipole Patch Radiation Pattern

The far field radiation pattern for the both arrangements are shown below in Fig.B.5 and Fig.B.6.

The fabricated hardware models for linear and circular arrangement of 5 dipole patch elements. The fabricated models are shown in below figures. Figures (B.7, B.8) shows fabricated images of the linear arrangement of 5 dipole front view and back view respectively, and figures (B.9, B.10) shows fabricated models of the circular arrangement of 5 dipole elements front and back views respectively.

These fabricated prototypes are tested using Wave and Antenna Training

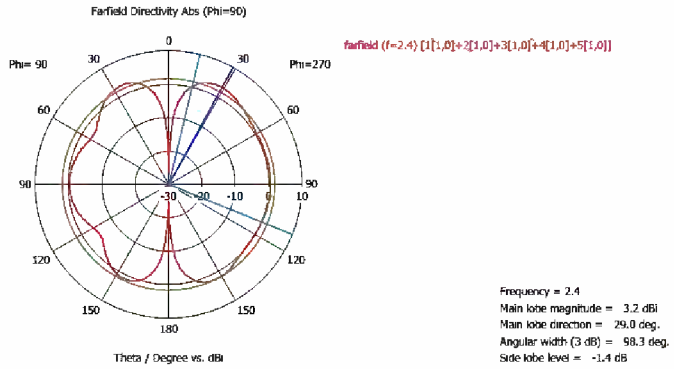

Figure B.6: Printed Circular Dipole Patch Radiation Pattern

Figure B.7: Fabricated Linear arrangement of 5 dipole antenna elements

Figure B.8: Fabricated Linear arrangement of 5 dipole antenna elements

Figure B.9: Fabricated Linear arrangement of 5 dipole antenna elements

Figure B.10: Fabricated Linear arrangement of 5 dipole antenna elements

Figure B.11: Linear printed dipole as transmitting antenna

System (WATS-2002). The testing process has been carried out by considering the prototypes in transmitting side as well as in receiving side. Different scenarios are considered for testing the prototype.

Case-I: Linear printed dipole patch antenna is considered as a transmitting antenna and a single dipole patch as receiver, the experimental setup is as shown in Fig.B.11. Radiation pattern is observed by using WATS-2002

Figure B.12: Observed radiation pattern for 0.2m distance of separation

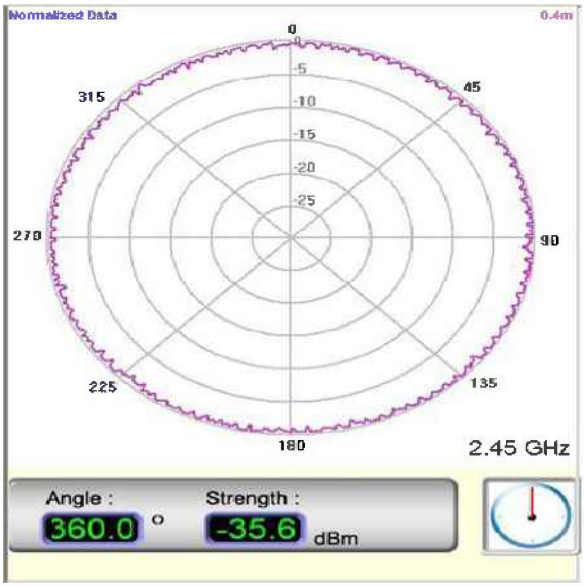

Figure B.13: Observed radiation pattern for 0.4m distance of separation

by considering distance of separation upto one meter in steps of 0.2 meters. The observed radiation pattern for different distances are as shown in figures B.12-B.16.

Case-II: In this scenario printed linear dipole is considered as a receiving antenna where a dipole patch is transmitting, and the experimental setup is as shown in Fig.B.17

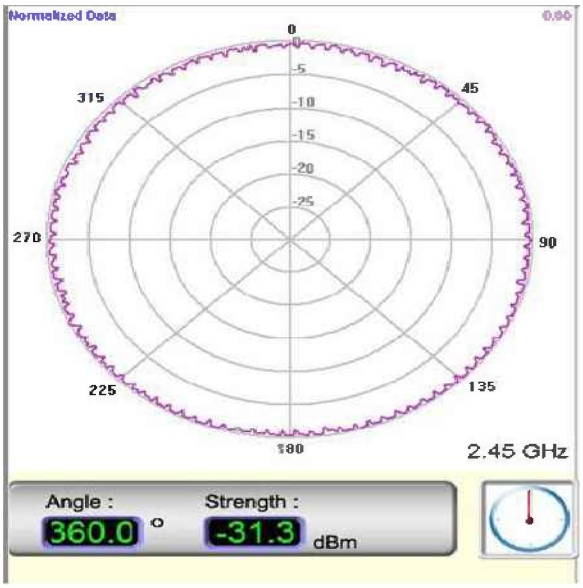

Figure B.14: Observed radiation pattern for 0.6m distance of separation

Figure B.15: Observed radiation pattern for 0.8m distance of separation

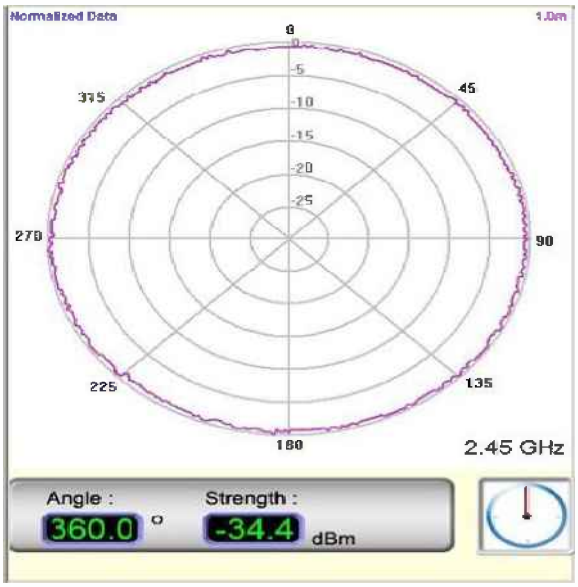

Figure B.16: Observed radiation pattern for 1m distance of separation

Figure B.17: Linear printed dipole as receiving antenna

Radiation pattern observed with printed dipole as a receiving antenna by considering distance of separation upto 1m insteps of 0.2m. The observed radiation patterns are as shown in figures B.18-B.22.

Case-III: In this case printed dipole antenna array with circular arrangement is considered as a transmitting antenna with dipole patch as receiver. And experimental setup for this case is as shown in Fig.B.23.

The observed radiation pattern for the different scenarios by varying the

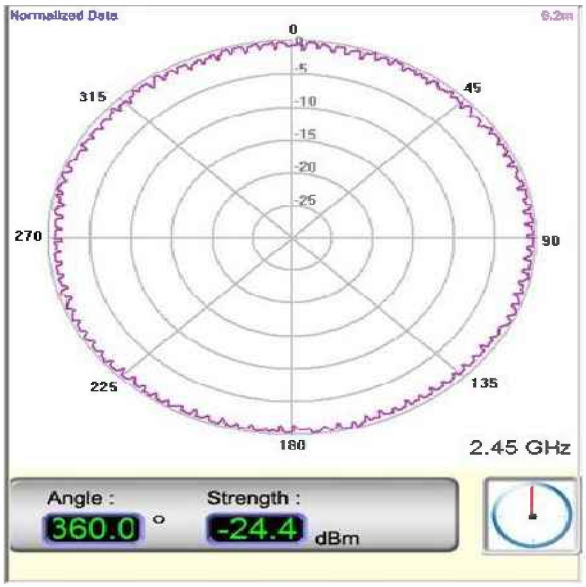

Figure B.18: Observed radiation pattern for 0.2m distance of separation

Figure B.19: Observed radiation pattern for 0.4m distance of separation

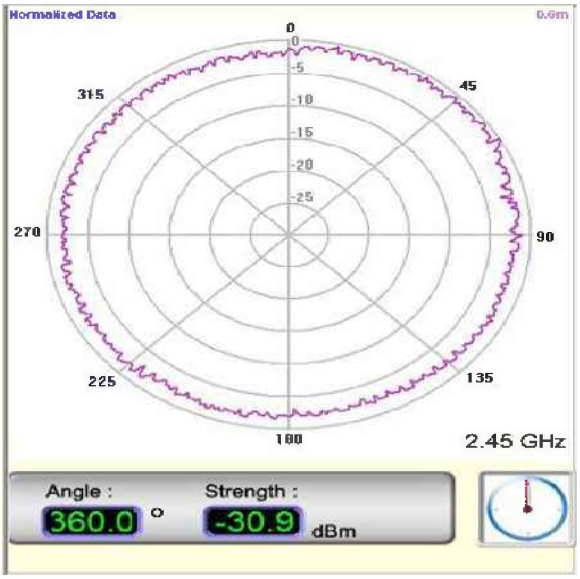

Figure B.20: Observed radiation pattern for 0.6m distance of separation

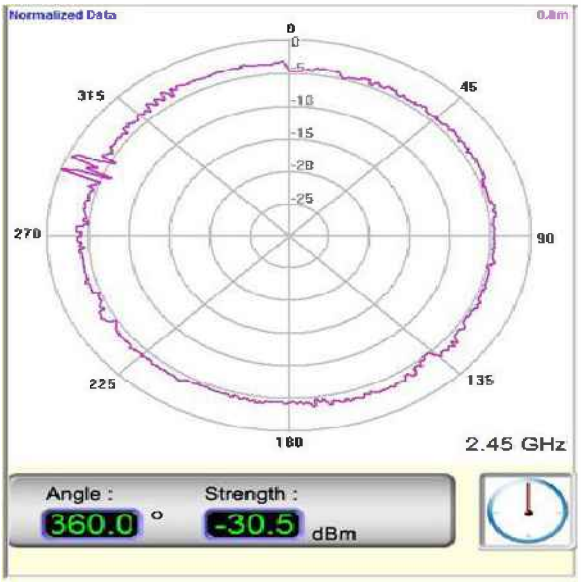

Figure B.21: Observed radiation pattern for 0.8m distance of separation

Figure B.22: Observed radiation pattern for 1m distance of separation

Figure B.23: Circular printed dipole as transmitting antenna

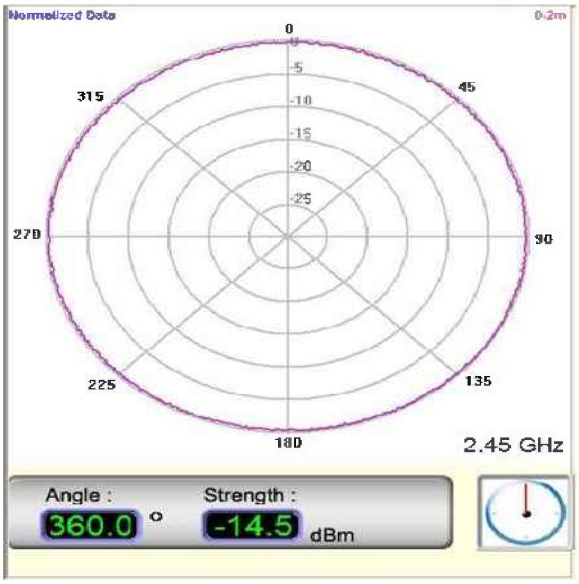

Figure B.24: Observed radiation pattern for 0.2m distance of separation

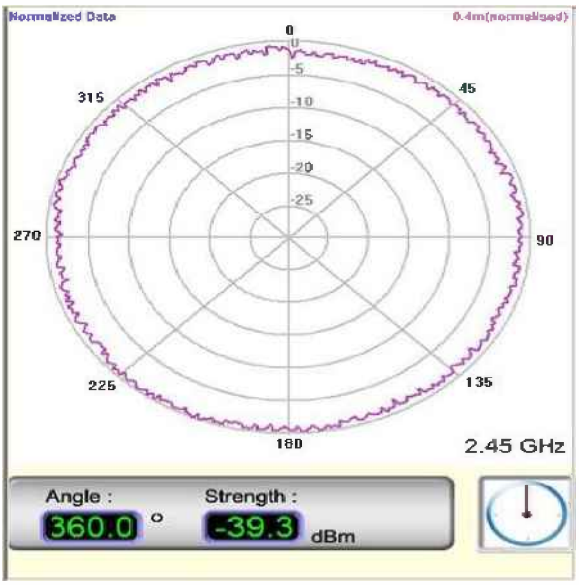

Figure B.25: Observed radiation pattern for 0.4m distance of separation

distance between transmitter and receiver are as shown in figuresB.24-B.28.

Case-IV: In this case printed circular arrangement of dipole antenna is considered as a receiving antenna and a single dipole as a transmitter, the experimental setup is as shown in Fig.B.29.

Radiation pattern is observed by using WATS-2002 and the observed ra-

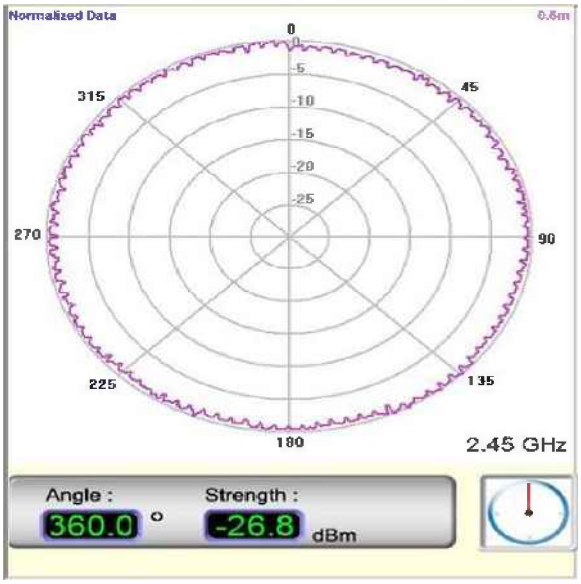

Figure B.26: Observed radiation pattern for 0.6m distance of separation

Figure B.27: Observed radiation pattern for 0.8m distance of separation

Figure B.28: Observed radiation pattern for 1m distance of separation

Figure B.29: Circular printed dipole as receiving antenna

Figure B.30: Observed radiation pattern for 0.2m distance of separation

Figure B.31: Observed radiation pattern for 0.4m distance of separation

diation patterns with the separation of 0.2m and increasing in steps of 0.2m upto a 1m distance are as shown in figures B.30-B.34.

The comparison of the strength of the each array in different roles like transmitter and receiver can be observed by plotting a graph with respect to the distance of separation and is shown below in Fig.B.35.

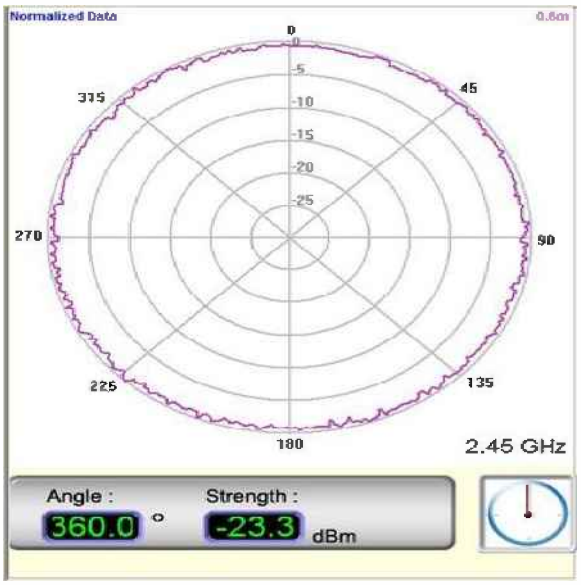

Figure B.32: Observed radiation pattern for 0.6m distance of separation

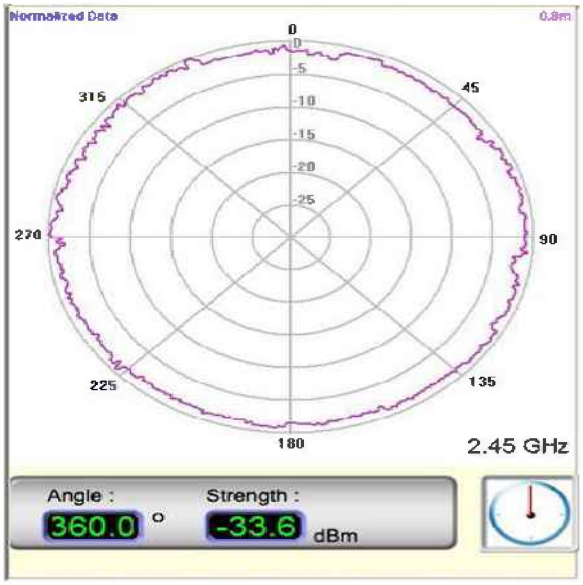

Figure B.33: Observed radiation pattern for 0.8m distance of separation

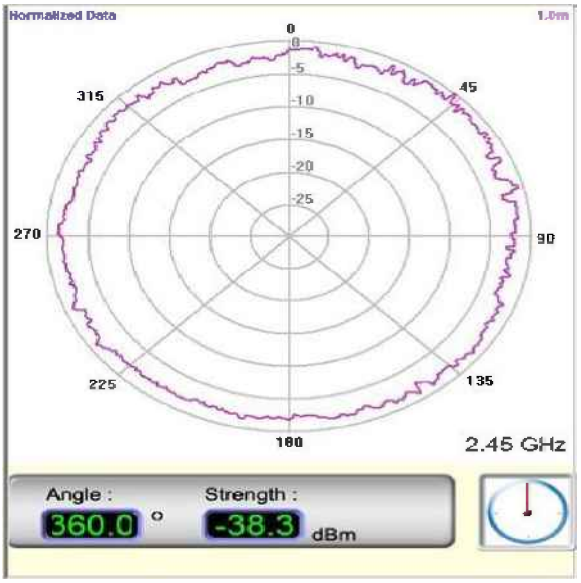

Figure B.34: Observed radiation pattern for 1m distance of separation

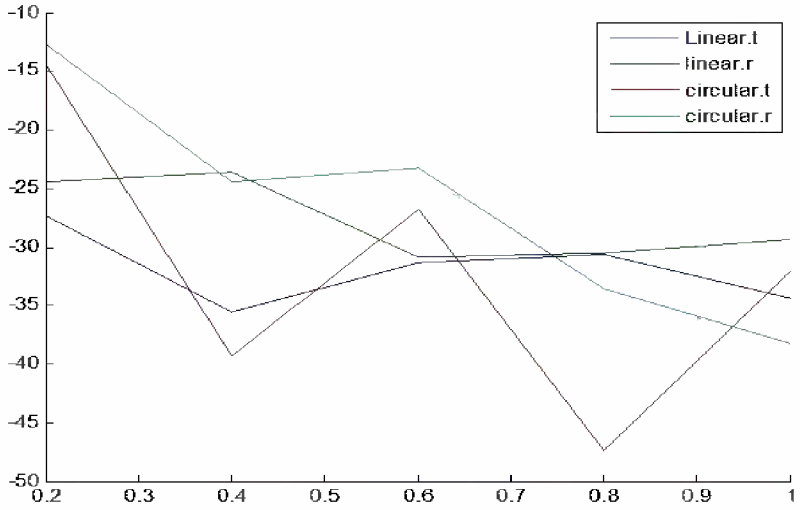

Figure B.35: Comparison of strength of each array in terms of distance

Publications From This Thesis

- **D.Suneel Varma**, *Design optimization analysis for multi-constraint adaptive antenna array using Harmony Search and Differential Evolution Techniques*, IEEE CONFERENCE ON INFORMATION AND COMMUNICATION TECHNOLOGIES(ICICT-2013), Apr-2013.
- **D.Suneel Varma**, *Synthesis of adaptive antenna with circular geometry employing Harmony Search and Differential Evolution techniques*, INTERNATIONAL CONFERENCE ON COMMUNICATION AND SIGNAL PROCESSING (ICCSP), Apr-2013.
- **D.Suneel Varma**, *Smart antenna Synthesis using improved evolutionary techniques*, communicated to Journal of Communication, Taylor and Fransic.